Journal of Multivariate Analysis 101 (2010) 1203–1225

Contents lists available at ScienceDirect

Journal of Multivariate Analysis

journal homepage: www.elsevier.com/locate/jmva

Universality in complex Wishart ensembles for general covariance matrices with 2 distinct eigenvalues[☆]

M.Y. Mo

School of Mathematics, University of Bristol, Bristol BS8 1TW, UK

ARTICLE INFO

Article history:
Received 6 February 2009
Available online 11 December 2009

AMS subject classifications:
primary 15A52
secondary 60F15
62H99

Keywords:
Wishart matrices
Phase transition
Riemann–Hilbert problem
Random matrix theory
Universality

ABSTRACT

We considered $N \times N$ Wishart ensembles in the class $W_{\mathbb{C}}(\Sigma_N, M)$ (complex Wishart matrices with M degrees of freedom and covariance matrix Σ_N) such that N_0 eigenvalues of Σ_N are 1 and $N_1 = N - N_0$ of them are a. We studied the limit as M, N, N_0 and N_1 all go to infinity such that $\frac{N}{M} \to c$, $\frac{N_1}{N} \to \beta$ and $0 < c, \beta < 1$. In this case, the limiting eigenvalue density can either be supported on 1 or 2 disjoint intervals in $\mathbb{R}_+$, and a phase transition occurs when the support changes from 1 interval to 2 intervals. By using the Riemann–Hilbert analysis, we have shown that when the phase transition occurs, the eigenvalue distribution is described by the Pearcey kernel near the critical point where the support splits.

1. Introduction

Let X be an $M \times N$ (assuming $M \geq N$) matrix with i.i.d. complex Gaussian entries whose real and imaginary parts have variance $\frac{1}{2}$ and zero mean. Let Σ_N be an $N \times N$ positive definite Hermitian matrix with eigenvalues $a_1 > \cdots > a_N$ (not necessarily distinct). In this paper, we will consider the case where Σ_N has only 2 distinct eigenvalues, 1 and a such that N_1 of its eigenvalues are a and $N - N_1$ of them are 1. We will assume that $\frac{N}{M} \to c$ and $\frac{N_1}{N} \to \beta$ as $N, M \to \infty$ and that $0 < c, \beta < 1$. To be precise, we will assume the following

$$cM - N = \tau_1 = O(1), \qquad N\beta - N_1 = \tau_2 = O(1), \quad M, N, N_1 \to \infty. \tag{1.1}$$

Let $\Sigma_N^{\frac{1}{2}}$ be any Hermitian square root of Σ_N. Then the columns of the matrix $X\Sigma_N^{\frac{1}{2}}$ are random vectors with variances $\frac{1}{2}\sqrt{a_j}$. Let the matrix B_N be the following

$$B_N = \frac{1}{M}\Sigma_N^{\frac{1}{2}} X^{\dagger} X \Sigma_N^{\frac{1}{2}}. \tag{1.2}$$

Then B_N is the sample covariance matrix of the columns of $X\Sigma_N^{\frac{1}{2}}$, while Σ_N is the covariance matrix. In particular, B_N is a complex Wishart matrix in the class $W_{\mathbb{C}}(\Sigma_N, M)$.

☆ The funding of this research is provided by the EPSRC grant EP/D505534/1.
E-mail address: m.mo@bristol.ac.uk.

0047-259X/$ – see front matter © 2009 Elsevier Inc. All rights reserved.
doi:10.1016/j.jmva.2009.12.004

The sample covariance matrix is a fundamental tool in the study of multivariate statistics and its distribution was already known to Wishart around 1928 (see e.g. [1])

$$\mathcal{P}(B_N) = \frac{1}{C} e^{-M\mathrm{tr}(\Sigma_N^{-1}B_N)} (\det B_N)^{M-N}, \quad M \geq N, \tag{1.3}$$

for some normalization constant C.

Let $y_1, \ldots, y_N > 0$ be the eigenvalues of the sample covariance matrix B_N. Suppose N_1 eigenvalues of Σ_N are a and $N - N_1$ are 1. Without loss of generality, we may assume $0 < a < 1$. Then the joint probability density function (j.p.d.f) for the eigenvalues of B_N is given by

$$\mathcal{P}(y) = \frac{1}{Z_{M,N}} \prod_{i<j}(y_i - y_j) \prod_{j=1}^{N} y_j^{M-N} \det \left[y_k^{d_j^N - 1} e^{-M a_j^{-1} y_k} \right]_{1 \leq j,k, \leq N}, \tag{1.4}$$

where $Z_{M,N}$ is a normalization constant and d_j^N, a_j are given by

$$\begin{aligned} &d_j^N = j, \qquad a_j = 1, \quad 1 \leq j \leq N - N_1, \\ &d_j^N = j - N + N_1, \qquad a_j = a, \quad N - N_1 < j \leq N. \end{aligned}$$

In this paper we will study the asymptotic limit of the Wishart distribution with $\frac{N}{M} \to c$ and $\frac{N_1}{N} \to \beta$ as $M, N \to \infty$ in such a way that $0 < \beta, c < 1$. In this case, the empirical distribution function (e.d.f) F_N of the eigenvalues will converge weakly to a nonrandom p.d.f. F, which will be supported on either 1 or 2 intervals in $\mathbb{R}_+$. By applying the results of [2] to our case, we can extract properties of the measure F from the solutions of an algebraic equation (see Section 3 for details)

$$\begin{aligned} &za\xi^3 + (A_2 z + B_2)\xi^2 + (z + B_1)\xi + 1 = 0, \\ &A_2 = (1 + a), \qquad B_2 = a(1 - c), \\ &B_1 = 1 - c(1 - \beta) + a(1 - c\beta). \end{aligned} \tag{1.5}$$

The results in [2] imply that the real zeros of the function $\frac{\mathrm{d}z(\xi)}{\mathrm{d}\xi}$ determine the boundary points of the support of F. Since the zeros of $\frac{\mathrm{d}z(\xi)}{\mathrm{d}\xi}$ coincide with the zeros of the following quartic polynomial,

$$\begin{aligned} &a^2(1 - c)\xi^4 + 2a^2(1 - c\beta) + a(1 - c(1 - \beta))\xi^3 \\ &\quad + (1 - c(1 - \beta) + a^2(1 - c\beta) + 4a)\xi^2 + 2(1 + a)\xi + 1 = 0, \end{aligned} \tag{1.6}$$

the real roots of (1.6) are important in the determination of Supp(F). In particular, if $\Delta < 0$, then the support of F consists of a single interval, and if $\Delta > 0$, then the support of F consists of 2 disjoint intervals (see Propositions 2 and 5).

Let γ_k be the zeros of the polynomial (1.6) and let λ_k be

$$\lambda_k = -\frac{1}{\gamma_k} + c\frac{1 - \beta}{1 + \gamma_k} + c\frac{a\beta}{1 + a\gamma_k}, \quad k = 1, \ldots, 4. \tag{1.7}$$

We will order the λ_k such that, if all λ_k are real ($\Delta > 0$), then $\lambda_1 < \cdots < \lambda_4$ and if only two λ_k are real ($\Delta < 0$), then $\lambda_1 < \lambda_2$ are real and $\lambda_3 = \overline{\lambda_4}$ are complex.

Then the distribution function F has a continuous density $F(z) = \rho(z)\mathrm{d}z$ that is supported on $[\lambda_1, \lambda_2] \cup [\lambda_3, \lambda_4]$ when $\Delta > 0$ and on $[\lambda_1, \lambda_2]$ when $\Delta < 0$. Near the end points, the density $\rho(z)$ vanishes like a square root.

$$\rho(z) = \frac{\rho_k}{\pi}|z - \lambda_k|^{\frac{1}{2}} + O\left((z - \lambda_k)\right), \quad z \to \lambda_k. \tag{1.8}$$

An open problem in the study of Wishart ensembles is the universality and the distribution of the largest eigenvalue. Although the Wishart distribution has been known for a long time, results on the universality and the largest eigenvalue distribution were only obtained recently [3–13]. An important result by Baik, Ben-Arous and Péché [4] shows that the m-point correlation functions of the eigenvalues can be expressed in terms of a kernel $K_{M,N}(x, y)$

$$\mathcal{R}_m^{(M,N)}(y_1, \ldots, y_m) = \det\left(K_{M,N}(y_j, y_k)\right)_{1 \leq j,k \leq m} \tag{1.9}$$

where $\mathcal{R}_m^{(M,N)}(y_1, \ldots, y_m)$ is the m-point correlation function

$$\mathcal{R}_m^{(M,N)}(y_1, \ldots, y_m) = \frac{N!}{(N - m)!} \int_{\mathbb{R}_+} \cdots \int_{\mathbb{R}_+} \mathcal{P}(y)\mathrm{d}y_{m+1} \ldots \mathrm{d}y_N. \tag{1.10}$$

Moreover, the kernel $K_{M,N}(x, y)$ can be written as

$$K_{M,N}(x, y) = \int_0^\infty I_{M,N}(x + u)J_{M,N}(u + y)\mathrm{d}u,$$

with $H_{M,N}$ and $J_{M,N}$ given by

$$I_{M,N}(x) = \frac{M}{2\pi}\int_{\Gamma} \mathrm{d}z \mathrm{e}^{-xM(z-q)} z^M \prod_{k=1}^{N} \frac{1}{a_k^{-1} - z},$$
$$J_{M,N}(x) = \frac{M}{2\pi}\int_{\Xi} \mathrm{d}w \mathrm{e}^{yM(w-q)} w^{-M} \prod_{k=1}^{N} (a_k^{-1} - w),$$

where $q \in \mathbb{R}$ is such that $0 < q < a_1^{-1}$ and the contour Ξ (Γ) is a simple closed contour oriented counterclockwise and encircling the point 0 (the points $a_1^{-1}, \ldots, a_N^{-1}$).

Then by writing the factor $\mathrm{e}^{-xM(z-q)} z^M \prod_{k=1}^{N} \frac{1}{a_k^{-1}-z}$ as

$$\mathrm{e}^{-xM(z-q)} z^M \prod_{k=1}^{N} \frac{1}{a_k^{-1} - z} = \det(\Sigma_N) \mathrm{e}^{M\left(-x(z-q)+\log z - \frac{N}{M}\int_{\mathbb{R}} \log(1-zs) \mathrm{d}H_N(s)\right)},$$

and by a similar expression for $\mathrm{e}^{yM(w-q)} w^{-M} \prod_{k=1}^{N} (a_k^{-1} - w)$, where $H_N(s)$ is the empirical distribution function for the eigenvalues of Σ_N, one can compute the large M, N limit of the integrals $I_{M,N}$ and $J_{M,N}$ using the saddle point method. This was done in [4] to study the phase transitions in the spiked models [10], in which Σ_N is a finite rank perturbation of the identity matrix. The method was used later by El Karoui [8] to show that for a large class of complex Wishart ensembles, the asymptotic distribution of the largest eigenvalue is given by the Tracy–Widom distribution. Although in [8], the saddle point analysis was done for points x and y near the largest edge point of the asymptotic spectrum of B_N, the same type of analysis can be used to compute the asymptotic kernel in the bulk and other edge points, as well as to study the critical case. This was done by Brézin and Hikami for the simpler 'Gaussian random matrix with external source' model (see e.g. [14,15]). However, different steepest descent contours will have to be considered in each of these situations. Although the case considered here is included in [8], the less direct Riemann–Hilbert approach used in this paper is useful in applications such as the computation of ensemble averages (see, e.g. [16]).

In [17,6], the authors have expressed this kernel in terms of multiple orthogonal polynomials (see Section 2 for details). In this paper, we computed the asymptotics of the correlation kernel in (1.9) through the asymptotics of multiple Laguerre polynomials. This gives the following theorem.

Theorem 1. *Let $\rho(z)$ be the density function of F. Then for any x_0 in the interior of the support of F and $m \in \mathbb{N}$, we have*

$$\lim_{N,M\to\infty} \left(\frac{1}{M\rho(x_0)}\right)^m \mathcal{R}_m^{(M,N)}\left(x_0 + \frac{u_1}{M\rho(x_0)}, \ldots, x_0 + \frac{u_m}{M\rho(x_0)}\right) = \det\left(\frac{\sin\pi(u_i - u_j)}{\pi(u_i - u_j)}\right)_{i,j=1}^m \tag{1.11}$$

uniformly for any $(u_1, \ldots, u_m)$ in compact subsets of $\mathbb{R}^m$.

On the other hand, let $x_0 = \lambda_k$, where $k = 1, 2$ when $\Delta < 0$ and $k = 1, \ldots, 4$ when $\Delta > 0$. Then for any $m \in \mathbb{N}$, we have

$$\begin{aligned}\lim_{N,M\to\infty} &\left(\frac{1}{(M\rho_k)^{\frac{2}{3}}}\right)^m \mathcal{R}_m^{(M,N)}\left(\lambda_k + (-1)^k \frac{u_1}{(M\rho_k)^{\frac{2}{3}}}, \ldots, \lambda_k + (-1)^k \frac{u_m}{(M\rho_k)^{\frac{2}{3}}}\right) \\ &= \det\left(\frac{\mathrm{Ai}(u_i)\mathrm{Ai}'(u_j) - \mathrm{Ai}'(u_i)\mathrm{Ai}(u_j)}{u_i - u_j}\right)_{i,j=1}^m,\end{aligned} \tag{1.12}$$

uniformly for any $(u_1, \ldots, u_m)$ in compact subsets of $\mathbb{R}^m$, where $\mathrm{Ai}(z)$ is the Airy function and ρ_k, $k = 1, 2$ are the constants in (1.8).

Recall that the Airy function is the unique solution to the differential equation $v'' = zv$ that has the following asymptotic behavior as $z \to \infty$ in the sector $-\pi + \epsilon \le \arg(z) \le \pi - \epsilon$, for any $\epsilon > 0$.

$$\mathrm{Ai}(z) = \frac{1}{2\sqrt{\pi} z^{\frac{1}{4}}} \mathrm{e}^{-\frac{2}{3}z^{\frac{3}{2}}}\left(1 + O(z^{-\frac{3}{2}})\right), \quad -\pi + \epsilon \le \arg(z) \le \pi - \epsilon,\ z \to \infty \tag{1.13}$$

where the branch cut of $z^{\frac{3}{2}}$ in the above is chosen to be the negative real axis.

Note that the Airy kernel in (1.12), implies that the largest eigenvalue distribution is given by the Tracy–Widom distribution [18]. This is in agreement with the results in [8].

The main contribution of this paper is the study of the phase transition between the 1 cut case and the 2 cut case. When $\Delta = 0$ the eigenvalue density $\rho(z)$ becomes zero at a critical point λ_* in the interior of its support. In this case, a phase transition occurs and the local eigenvalue statistics near the critical point can be described by the Pearcey kernel. The behavior of the eigenvalues when the parameters a, $\beta_N = \frac{N_1}{N}$ and $c_N = \frac{N}{M}$ are such that $\Delta(a, \beta_N, c_N) = O\left(M^{-\frac{1}{2}}\right)$ can be studied by the techniques developed in [19]. In this case, there exist a_0, β_0 and c_0 such that the following

$$\begin{aligned} & a = a_0 + \frac{\eta_a}{M^{\frac{1}{2}}}, \qquad \beta_N = \beta_0 + \frac{\eta_\beta}{M^{\frac{1}{2}}}, \qquad c_N = c_0 + \frac{\eta_c}{M^{\frac{1}{2}}}, \\ & \Delta(a_0, \beta_0, c_0) = 0, \end{aligned} \tag{1.14}$$

are satisfied. There are many a_0, β_0 and c_0 such that (1.14) is satisfied. For the implementation of the techniques in [19], we also need the parameters a_0, β_0 and c_0 to satisfy the following

$$\mathcal{A}_2\gamma_*^2 + \mathcal{A}_1\gamma_* + \mathcal{A}_0 = 0, \tag{1.15}$$

where γ_* is the double root of (1.6) with parameters a_0, β_0 and c_0, and $\mathcal{A}_j$ are given by

$$\begin{aligned} \mathcal{A}_2 &= \frac{\eta_c}{M^{\frac{1}{2}}(c_0 - 1)}, \\ \mathcal{A}_1 &= \frac{1}{a_0(c_0 - 1)}\left(\chi_1 + \chi_2(a_0 - 1) + \frac{\eta_c}{M^{\frac{1}{2}}}(a_0 + 1)\right), \\ \mathcal{A}_0 &= \frac{1}{a_0(c_0 - 1)}\left(\chi_1 + \chi_2\left(1 - \frac{1}{a_0}\right) + \frac{\eta_c}{M^{\frac{1}{2}}}\right), \\ \chi_1 &= \left(1 - \frac{a_0}{a}\right)c_0\beta_0, \qquad \chi_2 = \left(1 - \frac{c_N(1 - \beta_N)}{c_0(1 - \beta_0)}\right)c_0(1 - \beta_0). \end{aligned} \tag{1.16}$$

In practice, to obtain the eigenvalue statistics, it is sufficient to solve a_0, β_0 and c_0 up to the order $O\left(M^{-1}\right)$. Since there are only 2 equations with 3 parameters, there may still be many solutions a_0, β_0 and c_0 that satisfy both (1.14) and (1.15). This reflects the fact that when $\Delta(a, \beta_N, c_N) = O\left(M^{-\frac{1}{2}}\right)$, the ensemble could be considered as perturbations to many different Wishart ensembles whose eigenvalue densities vanish inside its support.

Let ρ_*, υ_1 and υ_0 be the following constants

$$\begin{aligned} \rho_* &= \left(\frac{3\gamma_*^2(1 + \gamma_*)^2(1 + a_0\gamma_*)^2}{a_0^2(1 - c_0)(\gamma_* - \gamma_1)(\gamma_* - \gamma_2)}\right)^{\frac{1}{3}}, \\ \upsilon_1 &= \frac{1}{a_0(c_0 - 1)}\left(\frac{\eta_a c_0\beta_0}{a_0} + \left(c_0\eta_\beta - (1 - \beta_0)\eta_c\right)(a_0 - 1) + \eta_c(a_0 + 1)\right), \\ \upsilon_2 &= \frac{1}{a_0(c_0 - 1)}\left(\frac{\eta_a c_0\beta_0}{a_0} + \left(c_0\eta_\beta - (1 - \beta_0)\eta_c\right)\left(1 - \frac{1}{a_0}\right) + \eta_c\right) \end{aligned} \tag{1.17}$$

where γ_1 and γ_2 are the non-degenerate roots of Eq. (1.6) with parameters a_0, β_0 and c_0.

Then we see that $\mathcal{A}_1$ and $\mathcal{A}_0$ can be approximated by

$$\mathcal{A}_j = \frac{\upsilon_j}{M^{\frac{1}{2}}} + O(M^{-1}), \quad j = 0, 1. \tag{1.18}$$

We are now in a position to state our next result.

Theorem 2. *Suppose the discriminant Δ of (1.6) is of order $O\left(M^{-\frac{1}{2}}\right)$ for the parameters a, $\beta_N = \frac{N_1}{N}$ and $c = \frac{N}{M}$. Let a_0, β_0 and c_0 be a solution of (1.14) and (1.15) and let λ_* be the critical point in the spectrum that corresponds to the double root γ_* of (1.6) with parameters a_0, β_0 and c_0. Let t_0 be the following parameter*

$$t_0 = \frac{3\gamma_*^2(\gamma_* + 1)(2\eta_c\gamma_* + (1 - c_0)\upsilon_1)}{\rho_*^{\frac{3}{2}}(1 - c_0)(\gamma_* - \gamma_1)(\gamma_* - \gamma_2)}$$

where υ_1 is defined in (1.17).

Then for any $m \in \mathbb{N}$, we have

$$\begin{aligned} & \lim_{N,M\to\infty}\left(\frac{1}{(M\rho_*)^{\frac{3}{4}}}\right)^m \mathcal{R}_m^{(M,N)}\left(\lambda_* + \frac{u_1}{(M\rho_*)^{\frac{3}{4}}}, \ldots, \lambda_* + \frac{u_m}{(M\rho_*)^{\frac{3}{4}}}\right) \\ & \quad = \det\left(\frac{P_1(u_i)P_2''(u_j) - P_1'(u_i)P_2'(u_j) + P_1''(u_i)P_2(u_j) - t_0P_1(u_i)P_2(u_j)}{u_i - u_j}\right)_{i,j=1}^m, \end{aligned} \tag{1.19}$$

uniformly for any $(u_1, \ldots, u_m)$ *in compact subsets of* $\mathbb{R}^m$*, where* ρ_* *is defined in* (1.17) *and* $P_1(x)$*,* $P_2(x)$ *are the Pearcey integrals defined by*

$$P_1(x) = \frac{1}{2\pi}\int_{\mathbb{R}} e^{-\frac{1}{4}s^4 - \frac{t_0}{2}s^2 + isx}ds, \qquad P_2(x) = \frac{1}{2\pi}\int_{\Xi} e^{\frac{1}{4}s^4 + \frac{t_0}{2}s^2 + isx}ds$$

where Ξ *is the contour consisting of the rays* $\arg(z) = \pm\frac{\pi}{4}$ *and* $\pm\frac{3\pi}{4}$*, and they are oriented such that the lines* $\arg(z) = \frac{\pi}{4}$ *and* $\arg(z) = -\frac{3\pi}{4}$ *are pointing into the origin, while the other two lines are pointing out from the origin.*

Finally, when $c = 1 + O\left(M^{-1}\right)$, the origin becomes an edge of the spectrum and the asymptotics of the multiple Laguerre polynomials are described by the Bessel functions near the origin. By using the asymptotics of the multiple Laguerre polynomials obtained in [20], one obtains the following theorem.

Theorem 3. *Let* $M - N = \alpha = O(1)$ *as* $M, N \to \infty$*. Suppose* N *is even and that half of the eigenvalues of* Σ_N *are equal to* 1 *and the other half are equal to* a*. Then for all* $m \in \mathbb{N}$*, we have*

$$\begin{aligned}
&\lim_{M,N\to\infty}\left(\frac{1}{2N^2(1+a^{-1})}\right)^m R_m^{(M,N)}\left(\frac{u_1}{2N^2(1+a^{-1})}, \ldots, \frac{u_m}{2N^2(1+a^{-1})}\right) \\
&\quad = \det\left(\frac{\mathbb{J}_\alpha\left(\sqrt{u_i}\right)\sqrt{u_j}\mathbb{J}_\alpha'\left(\sqrt{u_j}\right) - \mathbb{J}_\alpha\left(\sqrt{u_j}\right)\sqrt{u_i}\mathbb{J}_\alpha'\left(\sqrt{u_i}\right)}{2(u_i - u_j)}\right)_{i,j=1}^m
\end{aligned} \tag{1.20}$$

uniformly for any $(u_1, \ldots, u_m)$ *in compact subsets of* $\mathbb{R}^m$*, where* $\mathbb{J}_\alpha(z)$ *is the Bessel function of order* α*.*

$$\mathbb{J}_\alpha(z) = \sum_{k=0}^{\infty}\frac{(-1)^k}{k!}\frac{1}{\Gamma(\alpha+k+1)}\left(\frac{z}{2}\right)^{2k+\alpha}. \tag{1.21}$$

In this case, there is also an analogue; the smallest eigenvalue distribution is given by the following theorem.

Theorem 4. *Let* y_N *be the smallest eigenvalue of* B_N*; then we have*

$$\lim_{M,N\to\infty}\mathbb{P}\left(y_N\left(2N^2(1+a^{-1})\right)^{\frac{1}{2}} < s\right) = TW_0(s), \tag{1.22}$$

where $TW_0(s)$ *is the distribution*

$$TW_0(s) = 1 - \exp\left(-\frac{1}{4}\int_0^s \log\left(\frac{s}{t}\right)q_\alpha(t)dt\right),$$

and $q_\alpha(s)$ *is the solution of the Painlevé V equation*

$$s(q_\alpha^2 - 1)\left(sq_\alpha'\right)' = q_\alpha\left(sq_\alpha'\right)^2 + \frac{1}{4}(s-\alpha)^2 q_\alpha + \frac{1}{4}sq_\alpha^3\left(q_\alpha^2 - 2\right),$$

with the following asymptotic behavior as $s \to \infty$*.*

$$q_\alpha(s) \sim \frac{1}{2^\alpha\Gamma(1+\alpha)}s^{\frac{\alpha}{2}}, \quad s \to 0.$$

This result can be found in [21].

The results obtained in this paper are obtained through the Riemann–Hilbert analysis. In obtaining these results, we have to overcome certain technical difficulties, which we will explain now.

As in [22,23,20], a Riemann surface of the form (1.5) is essential to the implementation of the Riemann–Hilbert analysis. In the case $\Delta < 0$, one also needs to know the zero set of a real function $h(x)$. This function $h(x)$ is given as follows. If we express the solutions ξ in (1.5) as analytic functions of z, then the three solutions to (1.5) behave as follows when $z \to \infty$.

$$\begin{aligned}
&\xi_1(z) = -\frac{1}{z} + O(z^{-2}), \quad z \to \infty, \\
&\xi_2(z) = -1 + \frac{c(1-\beta)}{z} + O(z^{-2}), \quad z \to \infty, \\
&\xi_3(z) = -\frac{1}{a} + \frac{c\beta}{z} + O(z^{-2}), \quad z \to \infty.
\end{aligned} \tag{1.23}$$

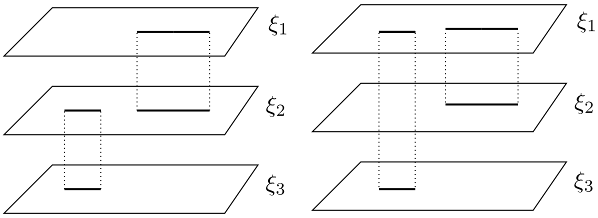

Fig. 1. Possible sheet structures of the Riemann surface when $\Delta > 0$. For the implementation of the Riemann–Hilbert analysis, we need to show that the Riemann surface has the sheet structure shown on the right hand side.

Then the function $h(x)$ is defined by

$$h(x) = \mathrm{Re}\left(\int_{\lambda_3}^{x} \xi_2(z) - \xi_3(z)\mathrm{d}z\right). \tag{1.24}$$

In order to implement the Riemann–Hilbert analysis, we must determine the sheet structure of the Riemann surface (1.5) and the topology of the zero set $\mathfrak{H}$ of $h(x)$. Since our model depends on three parameters c, a and β, while the models in [22,23,20] depend only on one parameter a, the determination of both the sheet structure of the Riemann surface and the topology of $\mathfrak{H}$ is considerably more difficult in our case and a large part of this paper is devoted to resolving these difficulties so that the Riemann–Hilbert analysis like those in [22,23,20] can be applied.

To determine the sheet structure of (1.5), note that although the number of real and complex branch points on the Riemann surface is known, it is unclear which Riemann sheet these branch points belong to, and different situations will result in different sheet structures of the Riemann surface as indicated in Fig. 1. In order to determine the sheet structure of the Riemann surface, we need to analyze the analyticity of the solutions ξ_j in the vicinity of the points λ_k in (1.7). This requires the type of analysis used in [24], which is very difficult to carry out in our case. In this paper, we overcome these difficulties by showing that the Stieltjes transform of the limiting eigenvalue distribution satisfies (1.5). Then by using properties of the Stieltjes transform obtained in [2,25–28], we were able to determine the sheet structure of the Riemann surface (1.5).

In the case when $\Delta < 0$, we also have to determine the topology of the zero set of $h(x)$. This is also more complicated than the models in [23,20] and a thorough analysis of this set making use of properties of harmonic functions is carried out in Section 3.4.1.

In the critical case, the Riemann surface in (1.5) will have to be modified before the Riemann–Hilbert analysis can be implemented. This was done in [19] for the simpler 'Gaussian random matrix with external source' model. However, in the case of complex Wishart ensembles, the Riemann surface has to be modified in a different way. This is discussed in Section 3.5. The present case also requires a more delicate error analysis than the case in [19]. This is explained in Section 4.

2. Multiple Laguerre polynomials and the correlation kernel

The main tool in our analysis involves the use of multiple orthogonal polynomials and their Riemann–Hilbert problems. In this section we shall recall the results in [17,6] and express the correlation kernel $K_{M,N}(x,y)$ in (1.9) in terms of multiple Laguerre polynomials. In Section 4, we will apply the Riemann–Hilbert analysis to obtain the asymptotics of these multiple Laguerre polynomials and use them to prove Theorems 1 and 2.

We shall not define the multiple Laguerre polynomials in the most general setting, but only define the ones that are relevant to our setup. Readers who are interested in the theory of multiple orthogonal polynomials can consult the papers [29,30,17,31]. Let $L_{n_1,n_2}(x)$ be the monic polynomial such that

$$\begin{aligned} &\int_0^\infty L_{n_1,n_2}(x)x^{i+M-N}\mathrm{e}^{-Mx}\mathrm{d}x = 0, \quad i = 0,\ldots,n_1-1, \\ &\int_0^\infty L_{n_1,n_2}(x)x^{i+M-N}\mathrm{e}^{-Ma^{-1}x}\mathrm{d}x = 0, \quad i = 0,\ldots,n_2-1 \end{aligned} \tag{2.1}$$

and let $Q_{n_1,n_2}(x)$ be a function of the form

$$Q_{n_1,n_2}(x) = A^1_{n_1,n_2}(x)\mathrm{e}^{-Mx} + A^a_{n_1,n_2}(x)\mathrm{e}^{-Ma^{-1}x}, \tag{2.2}$$

where $A^1_{n_1,n_2}(x)$ and $A^a_{n_1,n_2}(x)$ are polynomials of degrees n_1-1 and n_2-1, respectively, and $Q_{n_1,n_2}(x)$ satisfies the following

$$\int_0^\infty x^i Q_{n_1,n_2}(x)x^{M-N}\mathrm{d}x = \begin{cases} 0, & i = 0,\ldots,n_1+n_2-2; \\ 1, & i = n_1+n_2-1. \end{cases} \tag{2.3}$$

The polynomial $L_{n_1,n_2}(x)$ is called the multiple Laguerre polynomial of type II and the polynomials $A^1_{n_1,n_2}(x)$ and $A^a_{n_1,n_2}(x)$ are called multiple Laguerre polynomials of type I (with respect to the weights $x^{M-N}\mathrm{e}^{-Mx}$ and $x^{M-N}\mathrm{e}^{-Ma^{-1}x}$) [29,30]. These polynomials exist and are unique. Moreover, they admit integral expressions [17].

Let us define the constants $h^{(1)}_{n_1,n_2}$ and $h^{(2)}_{n_1,n_2}$ to be

$$\begin{aligned} h^{(1)}_{n_1,n_2} &= \int_0^\infty L_{n_1,n_2}(x)x^{n_1+M-N}\mathrm{e}^{-Mx}\mathrm{d}x, \\ h^{(2)}_{n_1,n_2} &= \int_0^\infty L_{n_1,n_2}(x)x^{n_2+M-N}\mathrm{e}^{-Ma^{-1}x}\mathrm{d}x. \end{aligned} \tag{2.4}$$

Then the following result in [17,6] allows us to express the correlation kernel in (1.9) in terms of a finite sum of multiple Laguerre polynomials.

Proposition 1. *The correlation kernel in $K_{M,N}(x,y)$ (1.9) can be expressed in terms of multiple Laguerre polynomials as follows*

$$\begin{aligned} (xy)^{\frac{N-M}{2}}(x-y)K_{M,N}(x,y) &= L_{N_0,N_1}(x)Q_{N_0,N_1}(x) - \frac{h^{(1)}_{N_0,N_1}}{h^{(1)}_{N_0-1,N_1}}L_{N_0-1,N_1}(x)Q_{N_0+1,N_1}(x) \\ &\quad - \frac{h^{(2)}_{N_0,N_1}}{h^{(2)}_{N_0,N_1-1}}L_{N_0,N_1-1}(x)Q_{N_0,N_1+1}(x) \end{aligned} \tag{2.5}$$

where $N_0 = N - N_1$.

This result allows us to compute the limiting kernel once we obtain the asymptotics for the multiple Laguerre polynomials.

3. Stieltjes transform of the eigenvalue distribution

In order to study the asymptotics of the correlation kernel, we would need to know the asymptotic eigenvalue distribution of the Wishart ensemble (1.3). Let $F_N(x)$ be the empirical distribution function (e.d.f) of the eigenvalues of B_N (1.2). The asymptotic properties of $F_N(x)$ can be found by studying its Stieltjes transform.

The Stieltjes transform of a probability distribution function (p.d.f) $G(x)$ is defined by

$$m_G(z) = \int_{-\infty}^\infty \frac{1}{\lambda - z}\mathrm{d}G(x), \quad z \in \mathbb{C}^+ = \{z \in \mathbb{C} : \mathrm{Im}(z) > 0\}. \tag{3.1}$$

Given the Stieltjes transform, the p.d.f can be found by the inversion formula

$$G([a,b]) = \frac{1}{\pi}\lim_{\epsilon\to 0^+}\int_a^b \mathrm{Im}\,(m_G(s+\mathrm{i}\epsilon))\,\mathrm{d}s. \tag{3.2}$$

The properties of the Stieltjes transform of $F_N(x)$ have been studied by Bai, Silverstein and Choi in the papers [2,25–28]. We will now summarize the results that we need from these papers.

First let us denote the e.d.f of the eigenvalues of Σ_N by H_N and assume that as $N \to \infty$, the distribution H_N weakly converges to a distribution function H. Let us then consider the matrix $\underline{B}_N$

$$\underline{B}_N = \frac{1}{N}X\Sigma_N X^\dagger. \tag{3.3}$$

The matrix $\underline{B}_N$ has the same eigenvalues as B_N together with an additional $M - N$ zero eigenvalues. Let the e.d.f of the eigenvalues of $\underline{B}_N$ be $\underline{F}_N$.

Then as $N \to \infty$, the e.d.f $\underline{F}_N(x)$ converges weakly to a nonrandom p.d.f $\underline{F}$, and the Stieltjes transform $m_{\underline{F}}$ of $\underline{F}(x)$ satisfies the following equation [2,28,26,27]

$$z(m_{\underline{F}}) = -\frac{1}{m_{\underline{F}}} + c\int_{\mathbb{R}} \frac{t}{1+tm_{\underline{F}}}\mathrm{d}H(t). \tag{3.4}$$

The points where $\frac{\mathrm{d}z(\xi)}{\mathrm{d}\xi} = 0$ are of significant interest to us as they are potential end points of the support of $\underline{F}$, due to the following result by Choi and Silverstein.

Lemma 1 *([2] See also [5]). Let G be a distribution whose Stieltjes transform satisfies*

$$z(m_G) = -\frac{1}{m_G} + c_G\int_{\mathbb{R}} \frac{t}{1+tm_G}\mathrm{d}H_G(t) \tag{3.5}$$

for some constant c_G and distribution $H_G(t)$. Then if $z \notin \mathrm{Supp}(G)$, $m = m_G(z)$ will satisfy the following.

1. $m \in \mathbb{R} \setminus \{0\}$;
2. $-\frac{1}{m} \notin \text{Supp}(H_G)$;
3. *Let z be defined by (3.4), and then $z'(m) > 0$, where the prime denotes the derivative with respect to m_G in (3.5).*

Conversely, if m satisfies 1–3, *then* $z = z(m) \notin \text{Supp}(G)$.

This lemma allows us to identify the complement of $\text{Supp}(\underline{F})$ by studying the real points m such that $z'(m) > 0$.

3.1. The Riemann surface and the Stieltjes transform

We will now restrict ourselves to the case when the matrix Σ_N has 2 distinct eigenvalues only. Without loss of generality, we will assume that one of these values is 1 and the other one is $0 < a < 1$. Let $0 < \beta < 1$; we will assume that as $N \to \infty$, N_1 of the eigenvalues take the value a and $N_0 = N - N_1$ of the eigenvalues are 1 and that $\frac{N_1}{N} \to \beta$.

For the implementation of the Riemann–Hilbert analysis, it is more convenient to consider a measure $\hat{F}_N$ instead of the measure $\underline{F}$.

Let $c_N = \frac{N}{M}$ and $H_N(t)$ be the e.d.f

$$\mathrm{d}H_N(t) = (1 - \beta_N)\delta_1 + \beta_N \delta_a$$

where $\beta_N = \frac{N_1}{N}$.

Then $\hat{F}_N$ is the measure whose Stieltjes transform $m_N(z) = m_{\hat{F}_N}(z)$ is the unique solution of

$$z(m_N) = -\frac{1}{m_N} + c_N \int_{\mathbb{R}} \frac{t}{1 + t m_N} \mathrm{d}H_N(t) \tag{3.6}$$

in $\mathbb{C}^+$ that behaves like $-\frac{1}{z}$ as $z \to \infty$. Note that, as pointed out in [5], the measure $\hat{F}_N$ is not the eigenvalue distribution for finite N, instead, it is only defined through Eq. (3.6). From (3.6), we see that $m_N(z)$ is a solution of the algebraic equation

$$\begin{aligned} &za\xi^3 + (A_2 z + B_2^N)\xi^2 + (z + B_1^N)\xi + 1 = 0, \\ &A_2 = (1 + a), \qquad B_2^N = a(1 - c_N), \\ &B_1^N = 1 - c(1 - \beta_N) + a(1 - c_N \beta_N). \end{aligned} \tag{3.7}$$

This defines a Riemann surface $\mathcal{L}_N$ as a 3-folded cover of the complex plane.

In particular, these solutions have the behavior given by (1.23) as $z \to \infty$. On the other hand, as $z \to 0$, the 3 branches of $\xi(z)$ behave as follows

$$\begin{aligned} &\xi_\alpha^N(z) = -\frac{1 - c_N}{z} + O(1), \quad z \to 0, \\ &\xi_\beta^N(z) = R_1 + O(z), \quad z \to 0, \\ &\xi_\gamma^N(z) = R_2 + O(z), \quad z \to 0, \end{aligned} \tag{3.8}$$

where the order of the indices α, β and γ does not necessarily coincide with the ones in (1.23) (i.e. we do not necessarily have $\alpha = 1$, $\beta = 2$ and $\gamma = 3$). The constants R_1 and R_2 are the two roots of the quadratic equation

$$a(1 - c_N)x^2 + (1 - c_N(1 - \beta_N) + a(1 - c_N \beta_N))x + 1 = 0. \tag{3.9}$$

The functions $\xi_j^N(z)$ will not be analytic at the branch points of $\mathcal{L}_N$ and they will be discontinuous across the branch cuts joining these branch points. Moreover, from (3.8), one of the functions $\xi_j^N(z)$ will have a simple pole at $z = 0$. Apart from these singularities, however, the functions $\xi_j^N(z)$ are analytic.

3.2. Sheet structure of the Riemann surface

In this section we will study the sheet structure of the Riemann surface $\mathcal{L}_N$. As we shall see, the branch $\xi_1^N(z)$ turns out to be the Stieltjes transform $m_N(z)$ and its branch cut will be the support of $\hat{F}_N$.

By Lemma 1, the real points at which $\frac{\mathrm{d}z}{\mathrm{d}\xi} = 0$ characterize the end points of $\text{Supp}(\hat{F}_N)$. To determine the support, let us differentiate (3.7) to obtain an expression of $\frac{\mathrm{d}z}{\mathrm{d}\xi}$ in terms of ξ.

$$\begin{aligned} \frac{\mathrm{d}z}{\mathrm{d}\xi} = &\frac{1}{\xi^2(1+\xi)^2(1+a\xi)^2} \left(a^2(1 - c_N)\xi^4 + 2a^2(1 - c_N\beta_N) + a(1 - c_N(1 - \beta_N))\xi^3 \right. \\ &\left. + \ (1 - c_N(1 - \beta_N) + a^2(1 - c_N\beta_N) + 4a)\xi^2 + 2(1 + a)\xi + 1\right). \end{aligned} \tag{3.10}$$

In particular, the values of ξ at $\frac{dz}{d\xi}=0$ correspond to the roots of the quartic equation

$$\begin{aligned} &a^2(1-c_N)\xi^4+2a^2(1-c_N\beta_N)+a(1-c_N(1-\beta_N))\xi^3\\ &\quad+(1-c_N(1-\beta_N)+a^2(1-c_N\beta_N)+4a)\xi^2+2(1+a)\xi+1=0. \end{aligned} \tag{3.11}$$

Let Δ_N be the discriminant of this quartic polynomial. We shall consider the case where $\lim_{N\to\infty}\Delta_N>0$ and $\lim_{N\to\infty}\Delta_N<0$ separately and denote the case $\lim_{N\to\infty}\Delta_N>0$ by the '2 cut case' and the case $\lim_{N\to\infty}\Delta_N<0$ by the '1 cut case'.

3.3. Sheet structure in the 2 cut case

When $\Delta_N>0$, Eq. (3.11) will have 4 distinct real roots $\gamma_1^N<\cdots<\gamma_4^N$. Since $0<c_N,\beta_N<1$, the coefficients of (3.11) are all positive and hence all γ_k^N are negative.

Let λ_k^N be the corresponding points in the z-plane

$$\lambda_k^N=-\frac{1}{\gamma_k^N}+c_N\frac{1-\beta_N}{1+\gamma_k^N}+c_N\frac{a\beta_N}{1+a\gamma_k^N},\quad k=1,\ldots,4. \tag{3.12}$$

Note that, from the behavior of $z(\xi)$ in (3.7), we see that near the points -1 and $-\frac{1}{a}$, the function $z(\xi)$ behaves as

$$\begin{aligned} z(\xi)&=\frac{c_N(1-\beta_N)}{1+\xi}+O(1),\quad \xi\to-1,\\ z(\xi)&=\frac{c_Na\beta_N}{1+a\xi}+O(1),\quad \xi\to-\frac{1}{a} \end{aligned} \tag{3.13}$$

and hence $z'(\xi)$ is negative near these points. From this and (3.10), we see that $z'(\xi)>0$ on the intervals $(-\infty,\gamma_1^N)$, (γ_2^N,γ_3^N), $(\gamma_4^N,0)$ and $(0,\infty)$ and none of the points -1 and $-\frac{1}{a}$ belongs to these intervals. On (γ_1^N,γ_2^N) and (γ_3^N,γ_4^N), $z'(\xi)$ is negative. In particular, both $z(\xi)$ and $z'(\xi)$ are continuous on these intervals while $z(\xi)$ is strictly increasing. This implies the following.

Lemma 2. *The intervals $(-\infty,\gamma_1^N)$, (γ_2^N,γ_3^N), $(\gamma_4^N,0)$ and $(0,\infty)$ are mapped by $z(\xi)$ to $(0,\lambda_1^N)$, $(\lambda_2^N,\lambda_3^N)$, (λ_4^N,∞) and $(-\infty,0)$ respectively. Furthermore, we have $\lambda_2^N<\lambda_3^N$.*

Therefore the complement of $\mathrm{Supp}(\underline{F})$ is given by (recall that $\underline{F}$ has a point mass at 0)

$$\mathrm{Supp}(\hat{F}_N)^c=(-\infty,0)\cup(0,\lambda_1^N)\cup(\lambda_2^N,\lambda_3^N)\cup(\lambda_4^N,\infty). \tag{3.14}$$

Thus if $\lambda_1^N<\lambda_2^N$ and $\lambda_3^N<\lambda_4^N$, the support of $\hat{F}_N$ will consist of the 2 intervals $[\lambda_1^N,\lambda_2^N]$ and $[\lambda_3^N,\lambda_4^N]$. We would like to show that whenever $\Delta_N>0$, we have $\lambda_1^N<\lambda_2^N<\lambda_3^N<\lambda_4^N$.

The λ_k^N are the z-coordinates of the zeros of $z'(\xi)$ on $\mathcal{L}_N$. We can treat (3.7) as a polynomial in ξ; then λ_k^N will be the zeros of its discriminant $D_3^N(z)=(1-a)^2\prod_{j=1}^4(z-\lambda_j^N)$.

Let z_j^N be the jth smallest of the λ_k^N and let J be the union of the intervals $[z_1^N,z_2^N]$ and $[z_3^N,z_4^N]$. Since the leading coefficient of $D_3^N(z)$ is $(1-a)^2>0$, we see that the sign of $D_3^N(z)$ and hence the 3 roots of the cubic polynomial (3.7) behave as follows for $z\in\mathbb{R}$.

$$\begin{aligned} &1.\quad z\in\mathbb{R}\setminus J,\quad D_3^N(z)>0\Rightarrow \xi \text{ has 3 distinct real roots}\\ &2.\quad z\in J,\quad D_3^N(z)<0\Rightarrow \xi \text{ has 1 real and 2 complex roots.} \end{aligned} \tag{3.15}$$

In particular, the γ_j^N are the values of the double roots of the cubic polynomial (3.7) when $z=\lambda_j^N$. We then have the following lemma.

Lemma 3. *The points $-\frac{1}{a}\in[\gamma_1^N,\gamma_2^N]$ and $-1\in[\gamma_3^N,\gamma_4^N]$.*

Proof. Let us assume that none of the points -1 and $-\frac{1}{a}$ belongs to $[\gamma_1^N,\gamma_2^N]$. Then the function $z(\xi)$ is continuous on $[\gamma_1^N,\gamma_2^N]$. Moreover, from the behavior of z at these points (3.13), we see that none of them belongs to $[\gamma_2^N,\gamma_3^N]$ either and hence $z(\xi)$ is continuous on $[\gamma_1^N,\gamma_3^N]$. We have also seen in Lemma 2 that $\lambda_2^N<\lambda_3^N$. As the support of $\hat{F}_N$ is not empty, we have $\lambda_1^N<\lambda_4^N$. Now by the remark after (3.13), we see that $z'(\xi)$ is negative between γ_1^N and γ_2^N and hence we must have $\lambda_1^N>\lambda_2^N$ if $z(\xi)$ is continuous on $[\gamma_1^N,\gamma_2^N]$. Therefore we can either have $\lambda_3^N>\lambda_1^N>\lambda_2^N$ or $\lambda_1^N>\lambda_3^N>\lambda_2^N$. We will show that $z(\xi)$ cannot be continuous on $[\gamma_1^N,\gamma_3^N]$ in any of these cases.

Let us now assume $\lambda_3^N>\lambda_1^N>\lambda_2^N$. Then by (3.15) and the fact that $\lambda_1^N<\lambda_4^N$, we see that for $z_0\in[\lambda_2^N,\lambda_1^N]$, there is only one real m such that $z_0=z(m)$. However, by the continuity of $z(\xi)$ on the interval $[\gamma_1^N,\gamma_3^N]$, we see that there is at least one point on each of $[\gamma_1^N,\gamma_2^N]$ and $[\gamma_2^N,\gamma_3^N]$ that correspond to $z_0\in[\lambda_2^N,\lambda_1^N]$. This leads to a contradiction.

A similar consideration also leads to a contradiction to the case $\lambda_1^N > \lambda_3^N > \lambda_2^N$. This implies that $z(\xi)$ cannot be continuous on $[\gamma_1^N, \gamma_3^N]$.

By using the same argument, we can show that $z(\xi)$ cannot be continuous on $[\gamma_2^N, \gamma_4^N]$ either. This implies the lemma. □

We can now show that the points λ_k^N are ordered as $\lambda_1^N < \lambda_2^N < \lambda_3^N < \lambda_4^N$.

Lemma 4. *The λ_k^N satisfies $\lambda_1^N < \lambda_2^N < \lambda_3^N < \lambda_4^N$.*

Proof. As we have seen in the proof of Lemma 3, there are only 3 possible ways of ordering the points λ_1, λ_2^N and λ_3^N. Namely, $\lambda_3^N > \lambda_1^N > \lambda_2^N$, $\lambda_1^N > \lambda_3^N > \lambda_2^N$ or $\lambda_1^N < \lambda_2^N < \lambda_3^N$. We will show that the first two cases are not possible.

Let us assume $\lambda_3^N > \lambda_1^N > \lambda_2^N$. By Lemma 3, there is a singularity of $z(\xi)$ in $[\gamma_1^N, \gamma_2^N]$. Let us call this singularity s_0. Let $z_0 \in (\lambda_2^N, \lambda_1^N)$. By using the same continuity argument in the proof of Lemma 3, we see that there is at least a point on each of (γ_2^N, γ_3^N) and (s_0, γ_2^N) that correspond to z_0, which contradicts the fact that there can only be one real point m with $z(m) = z_0$. A similar argument shows that $\lambda_1^N > \lambda_3^N > \lambda_2^N$ is not possible either and hence we must have $\lambda_3^N > \lambda_2^N > \lambda_1^N$.

By carrying out the same argument for the points λ_2^N, λ_3^N and λ_4^N, we see that the only possible ordering of these points is $\lambda_2^N < \lambda_3^N < \lambda_4^N$. Hence we must have $\lambda_1^N < \lambda_2^N < \lambda_3^N < \lambda_4^N$. □

By Lemma 4 and the fact that when $\Delta_N \leq 0$, there can be at most 3 distinct real roots for Eq. (3.10), we obtain the following condition for the support to consist of 2 intervals.

Proposition 2. *Let Δ_N be the discriminant of the quartic polynomial (3.11); then the support of $\hat{F}_N$ consists of 2 disjoint intervals if and only if $\Delta_N > 0$.*

3.3.1. Branch cuts of the Riemann surface

In this section we will show that the solution $\xi_1^N(z)$ ((1.23) of (3.7)) coincides with the Stieltjes transform $m_N(z)$ in $\mathbb{C}^+ \cup \mathbb{R}$. Furthermore, when the support of $\hat{F}_N$ consists of 2 disjoint intervals, the function $\xi_1^N(z)$ and hence $m_N(z)$ will not be analytic at any of the points λ_k^N, $k = 1, \ldots, 4$.

The solutions $\xi_j^N(z)$ of (3.7) will not be analytic at the branch point $(\lambda_k^N, \gamma_k^N)$ if $\xi_j^N(\lambda_k^N) = \gamma_k^N$. Since all the λ_k^N are on the real axis and the only possible pole of these functions is at $z = 0$, there exist analytic continuations of the $\xi_j^N(z)$ in $\mathbb{C}^+$ that are continuous up to $\mathbb{R} \setminus \{0\}$.

Note that if λ_1^N (λ_3^N) is a branch point of $\xi_j^N(z)$, then for $z \in [\lambda_1^N, \lambda_2^N]$ ($[\lambda_3^N, \lambda_4^N]$), the function $\xi_j^N(z)$ is complex and will again be branched at λ_2^N (λ_4^N). Therefore we have the following lemma.

Lemma 5. *Let $\xi_j^N(z)$ be the solutions of (3.7) in $\left(\mathbb{C}^+ \cup \mathbb{R}\right) \setminus \{0\}$ that has the asymptotic behavior (1.23). Then for $j = 1, 2, 3$, $\xi_j^N(\lambda_1^N) = \gamma_1^N$ if and only if $\xi_j^N(\lambda_2^N) = \gamma_2^N$. Similarly, $\xi_j^N(\lambda_3^N) = \gamma_3^N$ if and only if $\xi_j^N(\lambda_4^N) = \gamma_4^N$.*

From the asymptotic behavior of the $\xi_j^N(z)$ (1.23) and the fact that the Stieltjes transform $m_N(z)$ solves (3.7) and vanishes as $z \to \infty$, we see that

$$m_N(z) = \xi_1^N(z), \quad z \in \left(\mathbb{C}^+ \cup \mathbb{R}\right) \setminus \{0\}. \tag{3.16}$$

Since $\hat{F}_N$ has a point mass of size $1 - c_N$ at zero, we see that $m_N(z)$, and hence $\xi_1^N(z)$, has the following singularity at $z = 0$.

$$\xi_1(z) = -\frac{1 - c_N}{z} + O(1), \quad z \to 0. \tag{3.17}$$

We will now show that for all λ_k^N, we have $\xi_1^N(\lambda_k^N) = \gamma_k^N$.

Proposition 3. *Let $\xi_1^N(z)$ be the solution of (3.7) in $\left(\mathbb{C}^+ \cup \mathbb{R}\right) \setminus \{0\}$ with the asymptotic behavior indicated as in (1.23). Then we have $\xi_1^N(\lambda_k^N) = \gamma_k^N$ for $k = 1, \ldots, 4$. In particular, $\xi_1^N(z)$ is not analytic at any of the points λ_k^N.*

Proof. Suppose for some λ_k^N we have $\xi_1^N(\lambda_k^N) \neq \gamma_k^N$ and that the support of $\hat{F}_N$ is on the left hand side of λ_k^N. Then we have $z'\left(\xi_1^N(\lambda_k^N)\right) \neq 0$. By Lemma 1, we must have $z'\left(m_N(\lambda_k^N + \delta)\right) > 0$ for small enough $\delta > 0$ as $\lambda_k^N + \delta$ does not belong to the support of $\hat{F}_N$ and m_N is real on $\lambda_k^N + \delta$. Then by continuity, we have $z'\left(m_N(\lambda_k^N)\right) > 0$. (As we assume, $z'\left(m_N(\lambda_k^N)\right) \neq 0$.)

Since $\xi_1^N(z)$ does not coincide with the double root of (3.7) at λ_k^N, it must be real in $[\lambda_k^N - \epsilon, \lambda_k^N + \epsilon]$ for some small $\epsilon > 0$. Therefore in this interval, $m_N(z)$ is real and $z'(m_N) > 0$. This implies that for some point $z_0 \in \mathrm{Supp}(\hat{F}_N)$, we have $z'(m_{\hat{F}_N}) > 0$ and $m_{\hat{F}_N} \in \mathbb{R} \setminus \{0, -1, -\frac{1}{a}\}$. This contradicts Lemma 1 and hence $\xi_1^N(\lambda_k^N) = \gamma_k^N$. By using exactly the same argument, we can prove the proposition for λ_k^N when the support lies on the right hand side of λ_k^N. □

This proposition implies that $\xi_1^N(z)$ is not analytic at the points λ_k^N for $k = 1, \ldots, 4$. We then have the following.

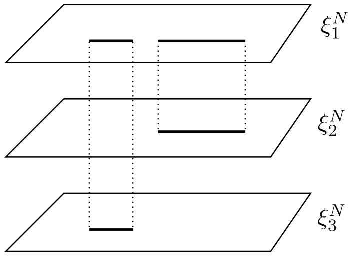

Fig. 2. The branch cut structure of the Riemann surface $\mathcal{L}_N$.

Proposition 4. *The function $\xi_3^N(z)$ has branch points at λ_1^N and λ_2^N while $\xi_2^N(z)$ has branch points at λ_3^N and λ_4^N.*

Proof. By using the asymptotic behavior of the branches $\xi_j^N(z)$ near infinity and zero, we see that $\xi_1^N > \xi_2^N > \xi_3^N$ for $z > \lambda_4^N$, while $\xi_3^N > \xi_2^N > \xi_1^N$ for $0 < z < \lambda_1^N$. Therefore ξ_1^N and ξ_2^N are branched at λ_4^N while ξ_1^N and ξ_3^N are branched at λ_1^N. By Lemma 5, we see that ξ_1^N and ξ_2^N are also branched at λ_3^N, while ξ_1^N and ξ_3^N are also branched at λ_2^N. □

We will now define the branch cuts of the function $\xi_1^N(z)$ to be $[\lambda_1^N, \lambda_2^N] \cup [\lambda_3^N, \lambda_4^N]$ and the branch cut for $\xi_2^N(z)$, $\xi_3^N(z)$ to be $[\lambda_3^N, \lambda_4^N]$, $[\lambda_1^N, \lambda_2^N]$ respectively. We then have the following relations between the ξ_j^N on the branch cuts

$$\xi_{1,\pm}^N(z) = \begin{cases} \xi_{2,\mp}^N(z), & z \in [\lambda_3^N, \lambda_4^N]; \\ \xi_{3,\mp}^N(z), & z \in [\lambda_1^N, \lambda_2^N] \end{cases} \tag{3.18}$$

where $\xi_{j,\pm}^N(z)$ indicates the boundary values of ξ_j^N on the $\pm$ sides of the branch cuts.

The branch cut structure of the Riemann surface $\mathcal{L}_N$ is indicated in Fig. 2. We will now define the functions $\theta_j^N(z)$ to be the integrals of $\xi_j^N(z)$.

$$\theta_1^N(z) = \int_{\lambda_4^N}^z \xi_1^N(x)\mathrm{d}x, \qquad \theta_2^N(z) = \int_{\lambda_4^N}^z \xi_2^N(x)\mathrm{d}x, \qquad \theta_3^N(z) = \int_{\lambda_2^N}^z \xi_3^N(x)\mathrm{d}x, \tag{3.19}$$

where the integration paths of the above integrals are chosen such that they do not intersect the real axis, except perhaps at the end points. Let us also define some constant shifts of the theta

$$\tilde{\theta}_1^N(z) = \theta_1^N(z), \qquad \tilde{\theta}_2^N(z) = \theta_2^N(z), \qquad \tilde{\theta}_3^N(z) = \theta_3^N(z) + \theta_{1,-}^N(\lambda_2^N). \tag{3.20}$$

These functions will be used in the Riemann–Hilbert analysis.

3.4. Sheet structure in the 1 cut case

We will now consider the case when $\Delta_N < 0$. In this case, Eq. (3.11) has 2 distinct real roots $\gamma_1^N < \gamma_2^N$ and 2 complex roots γ_3^N and $\gamma_4^N = \overline{\gamma}_3^N$. One can check that the coefficients of (3.11) are all positive and hence $\gamma_1^N < \gamma_2^N < 0$.

Then we have the following lemma.

Lemma 6. *The points λ_k^N, $k = 1, \ldots, 4$ are all distinct. In particular, $\lambda_3^N = \overline{\lambda}_4^N$ are not real.*

Proof. The points $(\lambda_k^N, \gamma_k^N)$, $k = 1, \ldots, 4$ are simple branch points of the Riemann surface $\mathcal{L}_N$. By considering the behavior of the functions $\xi(z)$ near these branch points, we see that if $\gamma_i^N \neq \gamma_j^N$ and $\lambda_i^N = \lambda_j^N$, there will be 4 distinct solutions $\xi(z)$ to Eq. (3.7) in a neighborhood of the point $\lambda_i^N = \lambda_j^N$, which is not possible. Therefore λ_i^N and λ_j^N are distinct. □

By using a similar argument that arrives at Lemma 2, we obtain the following lemma.

Lemma 7. *The intervals $(-\infty, \gamma_1^N)$, $(\gamma_2^N, 0)$ and $(0, \infty)$ are mapped by $z(\xi)$ to $(0, \lambda_1^N)$, (λ_2^N, ∞) and $(-\infty, 0)$ respectively. In particular, the complement of $\mathrm{Supp}(\hat{F}_N)$ is given by $\mathrm{Supp}(\hat{F}_N)^c = (-\infty, 0) \cup (0, \lambda_1^N) \cup (\lambda_2^N, \infty)$. Since the support of $\hat{F}_N$ is non-empty, we have $\lambda_1^N < \lambda_2^N$ and hence the support of $\hat{F}_N$ consists of a single interval.*

Therefore we have the following proposition.

Proposition 5. *Let Δ_N be the discriminant of the quartic polynomial (3.11); then if $\Delta_N < 0$, the support of $\hat{F}_N$ consists of a single interval.*

As in the 2 cut case, the function $\xi_1^N(z)$ is in fact the Stieltjes transform $m_N(z)$. Since $m_N(z)$ is the Stieltjes transform of a measure supported on the real axis, it is analytic away from the real axis and hence by (3.16), $\xi_1^N(z)$ is analytic at the points λ_3^N and λ_4^N with a branch cut on $[\lambda_1^N, \lambda_2^N]$. Since λ_3^N and λ_4^N are not branch points of the function $\xi_1^N(z)$, they must be branch points of the functions $\xi_2^N(z)$ and $\xi_3^N(z)$. This determines the branch structure of the Riemann surface $\mathcal{L}_N$. The branch cut of $\xi_2^N(z)$ and $\xi_3^N(z)$ will eventually be chosen to be a contour that goes from λ_4^N to λ_3^N intersecting the real axis at a point in $(\lambda_1^N, \lambda_2^N)$, but in the next section it will be chosen in a few different ways according to the situation.

3.4.1. Geometry of the problem in the 1 cut case

As explained in the Introduction, in the 1 cut case, the determination of the zero set of $h(x)$ in (1.24) is necessary for the implementation of the Riemann–Hilbert analysis. In this section we will carry out a thorough analysis of this set and determine its topology.

For the time being, we will choose the branch cut of $\xi_1^N(z)$ to be the interval $[\lambda_1^N, \lambda_2^N]$, and the branch cut between λ_3^N and λ_4^N to be a simple contour $\mathcal{C}$ that is symmetric with respect to the real axis and oriented upwards. Across $\mathcal{C}$, the two branches $\xi_2^N(z)$ and $\xi_3^N(z)$ change into each other. The branch cut $\mathcal{C}$ will be chosen such that it intersects the real axis at exactly one point x^* that is not equal to λ_1^N or λ_2^N.

We will now define the functions $\theta_j^N(z)$ to be the integrals of $\xi_j^N(z)$.

$$\theta_1^N(z) = \int_{\lambda_l^N}^{z} \xi_1^N(x)\mathrm{d}x, \qquad \theta_2^N(z) = \int_{\lambda_3^N}^{z} \xi_2^N(x)\mathrm{d}x, \qquad \theta_3^N(z) = \int_{\lambda_3^N}^{z} \xi_3^N(x)\mathrm{d}x,$$
$$\text{if } x^* < \lambda_2^N,\ l = 2;\ \text{if } x^* > \lambda_2^N,\ l = 1. \tag{3.21}$$

The integration paths of the above integrals are chosen as follows. If $x^* < \lambda_2^N$, then the integration path will not intersect the set $\mathcal{C} \cup (-\infty, \lambda_2^N)$ and if $x^* > \lambda_2^N$, then the integration path will not intersect the set $\mathcal{C} \cup (\lambda_1^N, \infty)$.

Then from (1.23), (3.8) and (3.17), we see that the integrals (3.21) have the following behavior at $z = \infty$ and $z = 0$.

$$\begin{aligned}
&\theta_1^N(z) = -\log z + l_1^N + O\left(z^{-1}\right), \quad z \to \infty,\\
&\theta_2^N(z) = -z + c_N(1-\beta_N)\log z + l_2^N + O\left(z^{-1}\right), \quad z \to \infty,\\
&\theta_1^N(z) = -(1-c_N)\log z + O(1), \qquad \theta_2^N(z) = O(1), \qquad \theta_3^N(z) = O(1), \quad z \to 0,\\
&\theta_3^N(z) = -\frac{z}{a} + c_N\beta_N \log z + l_3^N + O\left(z^{-1}\right), \quad z \to \infty,
\end{aligned} \tag{3.22}$$

for some constants l_1^N, l_2^N and l_3^N.

The set $\mathfrak{H}$ defined by

$$\mathfrak{H} = \left\{z \in \mathbb{C} |\ \mathrm{Re}\left(\theta_2^N(z) - \theta_3^N(z)\right) = 0\right\} \tag{3.23}$$

is important for the Riemann–Hilbert analysis. Let us now study its properties. Note that if $\xi(z)$ is a solution to (3.7), then so is $\overline{\xi}(\overline{z})$. In particular, by considering the behavior of $\xi_j(z)$ at infinity, we see that $\xi_j(z) = \overline{\xi}_j(\overline{z})$. This symmetry, together with the fact that $\xi_2(z)$ and $\xi_3(z)$ interchange across the branch cut $\mathcal{C}$, implies the following.

Lemma 8. *Let the branch cut $\mathcal{C}$ between λ_3^N and λ_4^N be a simple contour that is symmetric with respect to the real axis. Then the set $\mathfrak{H}$ in (3.23) is symmetric with respect to the real axis. Moreover, it is independent of the choice of the branch cut $\mathcal{C}$.*

We will now show that the real parts of $\xi_2^N(z)$ and $\xi_3^N(z)$ will coincide exactly once on the real axis.

Lemma 9. *Let x^* be the intersection between $\mathcal{C}$ and $\mathbb{R}$; then the real function* $\mathrm{Re}\left(\xi_2^N(z) - \xi_3^N(z)\right)$ *is continuous on $(-\infty, x^*)$ and (x^*, ∞) and it vanishes exactly once at a point $\iota \in \mathbb{R} \setminus \{x^*\}$.*

Proof. As $\mathrm{Re}\left(\xi_2^N(z) - \xi_3^N(z)\right)$ only changes sign across the point x^*, its zeros on $\mathbb{R}$ are independent of the location of x^*. Let us choose $\mathcal{C}$ such that $x^* < \lambda_1^N$.

By using a similar argument in the proof of Proposition 4, we see that $\xi_3^N(z) > \xi_2^N(z)$ on (x^*, λ_1^N), while $\xi_3^N(z) < \xi_2^N(z)$ for $z > \lambda_2^N$. Hence $\mathrm{Re}\left(\xi_2^N(z)\right)$ and $\mathrm{Re}\left(\xi_3^N(z)\right)$ must coincide at least once in $[\lambda_1^N, \lambda_2^N]$. We will show that they can only coincide once within $[\lambda_1^N, \lambda_2^N]$.

Inside $[\lambda_1^N, \lambda_2^N]$, the functions $\xi_1^N(z)$ and $\xi_2^N(z)$ become complex and are conjugate to each other. Since $\xi_{2,\pm}^N(z) = \xi_{1,\mp}^N(z)$ on $[\lambda_1^N, \lambda_2^N]$, while $\xi_3^N(z)$ has no jump discontinuity across $[\lambda_1^N, \lambda_2^N]$, we see that $\mathrm{Re}\left(\xi_2^N(z) - \xi_3^N(z)\right)$ is continuous on and across $[\lambda_1^N, \lambda_2^N]$. Therefore for $z \in \mathbb{R}$, this real function can only have jump discontinuity at the point x^*.

Taking the z-derivative of the coefficient of ξ^2 in (3.7), we obtain

$$3\frac{\mathrm{d}\xi_3^N(z)}{\mathrm{d}z} = \frac{1}{a}\frac{B_2^N}{z^2} - 2\frac{\mathrm{d}}{\mathrm{d}z}\mathrm{Re}\left(\xi_2^N(z) - \xi_3^N(z)\right).$$

From (3.7), it is easy to see that $B_2^N > 0$ as $c_N < 1$. Hence if the derivative of $\mathrm{Re}\left(\xi_2^N(z) - \xi_3^N(z)\right)$ is non-positive at a point $z_0 \in [\lambda_1^N, \lambda_2^N]$, we will have $\frac{\mathrm{d}\xi_3^N(z_0)}{\mathrm{d}z} > 0$. Since $\xi_3^N(z)$ is real, this would imply that the derivative $\frac{\mathrm{d}z(\xi)}{\mathrm{d}\xi}$ is positive at the real point $m = \xi_3^N(z_0)$. By Lemma 1, the point $z_0 = z(m)$ cannot belong to $\mathrm{Supp}\left(\hat{F}_N\right) = [\lambda_1^N, \lambda_2^N]$. This leads to a contradiction and hence we must have $\frac{\mathrm{d}}{\mathrm{d}z}\mathrm{Re}\left(\xi_2^N(z) - \xi_3^N(z)\right) > 0$ on $[\lambda_1^N, \lambda_2^N]$.

In particular, if the function $\mathrm{Re}\left(\xi_2^N(z) - \xi_3^N(z)\right)$ has more than one zero inside $[\lambda_1^N, \lambda_2^N]$, then at one of the zeros, its derivative must be smaller than or equal to zero. This is a contradiction and hence the function $\mathrm{Re}\left(\xi_2^N(z) - \xi_3^N(z)\right)$ can vanish at most once inside $[\lambda_1^N, \lambda_2^N]$. Therefore it must vanish exactly once inside $[\lambda_1^N, \lambda_2^N]$. This concludes the proof of the lemma. □

We can now determine the number of intersection points between $\mathfrak{H}$ and $\mathbb{R}$.

Lemma 10. *The set $\mathfrak{H}$ intersects $\mathbb{R}$ at most twice.*

Proof. By Lemma 9, the function $\mathrm{Re}\left(\xi_2^N - \xi_3^N\right)$ has exactly one zero on $\mathbb{R}$. This implies that $\mathrm{Re}(\theta_2^N - \theta_3^N)$ has only one turning point on $\mathbb{R}$ and hence $\mathfrak{H}$ can intersect $\mathbb{R}$ at most twice. □

We can now determine the shape of the set $\mathfrak{H}$.

Proposition 6. *The set $\mathfrak{H}$ consists of 4 simple curves, $\mathfrak{H}_\infty^\pm$, $\mathfrak{H}_L$ and $\mathfrak{H}_R$. The curve $\mathfrak{H}_\infty^+$ ($\mathfrak{H}_\infty^-$) is an open smooth curve that goes from λ_3^N (λ_4^N) to infinity. It approaches infinity in a direction parallel to the imaginary axis and does not intersect the real axis. The curves $\mathfrak{H}_L$ and $\mathfrak{H}_R$ are simple curves joining λ_3^N and λ_4^N. The curve $\mathfrak{H}_L$ is in the left hand side of $\mathfrak{H}_R$ and each of these curves intersects the real axis once. These two curves are smooth except at their intersections with the real axis. Let x_L and x_R be the intersection points of $\mathfrak{H}_L$ and $\mathfrak{H}_R$ with $\mathbb{R}$; then $(x_L, x_R) \cap [\lambda_1^N, \lambda_2^N] \neq \emptyset$.*

Proof. Let the sets $\mathfrak{H}_+$ and $\mathfrak{H}_-$ be the intersections of $\mathfrak{H}$ with the upper and lower half planes respectively. Then these 2 sets are reflections of each other with respect to the real axis. Within the set $\mathfrak{H}_+$, there are 3 curves $\mathfrak{H}_0^+$, $\mathfrak{H}_1^+$ and $\mathfrak{H}_2^+$ coming out of the point λ_3^N. Let us show that these curves are smooth except at λ_3^N. Suppose there is a point z_0 on $\mathfrak{H}_j^+$ that is not smooth. Since $\mathfrak{H}$ is independent of the choice of the branch cut $\mathfrak{C}$, by changing the branch cut if necessary, we can assume that both $\theta_2^N(z)$ and $\theta_3^N(z)$ are analytic at z_0. This means that the function $\theta_2^N - \theta_3^N$ is not conformal at z_0 and hence its derivative is zero at z_0. This would imply $\xi_2^N(z_0) = \xi_3^N(z_0)$ for $z_0 \neq \lambda_k^N$, which is not possible. Therefore the curves $\mathfrak{H}_j^+$, $j = 0, 1, 2$ are smooth except at the point λ_3^N.

Note that if there is a closed loop in $\mathfrak{H}$ that does not contain any of the points λ_k^N and does not intersect the branch cut $[\lambda_1^N, \lambda_2^N]$, the function $\mathrm{Re}\left(\theta_2^N - \theta_3^N\right)$ will be a constant inside this loop by the maximum modulus principle. This is not possible and therefore $\mathfrak{H}$ does not contain any closed loop of this type. In particular, the curves $\mathfrak{H}_j^+$ cannot be connected with one another except at the point λ_3^N.

By inspecting the behavior of $\theta_2^N - \theta_3^N$ at $z = \infty$, we see that one of the curves $\mathfrak{H}_j$ must be an open curve that approaches infinity at a direction parallel to the imaginary axis. We will call this curve $\mathfrak{H}_\infty^+$ and its reflection with respect to the real axis $\mathfrak{H}_\infty^-$. Since the other 2 curves cannot intersect each other, and they cannot go to infinity either, they must end at the real axis and be connected to the curves in $\mathfrak{H}^-$. We will call the curve on the left hand side $\mathfrak{H}_L^+$ and the one on the right hand side $\mathfrak{H}_R^+$. These two curves must end at different points on the real axis as they cannot intersect. Let us denote the curves $\mathfrak{H}_L$ and $\mathfrak{H}_R$ by

$$\mathfrak{H}_L = \mathfrak{H}_L^+ \cup \mathfrak{H}_L^- \cup \{x_L\}, \qquad \mathfrak{H}_R = \mathfrak{H}_R^+ \cup \mathfrak{H}_R^- \cup \{x_R\} \tag{3.24}$$

where $\mathfrak{H}_L^-$ and $\mathfrak{H}_R^-$ are the reflections of $\mathfrak{H}_L^+$ and $\mathfrak{H}_R^+$ with respect to the real axis, and x_L and x_R are their accumulation points on the real axis.

Let us now show that

$$\mathfrak{H}^+ = \mathfrak{H}_\infty^+ \cup \mathfrak{H}_L^+ \cup \mathfrak{H}_R^+. \tag{3.25}$$

Suppose there is a point $z_1 \in \mathfrak{H}^+$ that does not belong to any of the curves in the right hand side of (3.25). Then z_1 must belong to a curve $\mathfrak{H}_4^+ \in \mathfrak{H}^+$. By changing the definition of $\mathfrak{C}$ again if necessary, we see that $\mathfrak{H}_4^+$ must be smooth. This curve cannot end on the real axis because by Lemma 10, the set $\mathfrak{H}$ can at most intersect the real axis at 2 points and $\mathfrak{H}$ has already intersected the real axis at the 2 points x_L and x_R in (3.24). The curve $\mathfrak{H}_4^+$ cannot approach infinity or intersect any other curves in $\mathfrak{H}^+$ either and therefore it must be a closed loop in the upper half plane. This is not possible by the maximum modulus principle and hence we have

$$\mathfrak{H} = \mathfrak{H}_\infty^+ \cup \mathfrak{H}_\infty^- \cup \mathfrak{H}_L \cup \mathfrak{H}_R.$$

Finally, if $(x_L, x_R) \cap [\lambda_1^N, \lambda_2^N] = \emptyset$, then $\mathfrak{H}_L$ and $\mathfrak{H}_R$ will form a closed loop, which is forbidden by the maximum modulus principle. This concludes the proof of the proposition. □

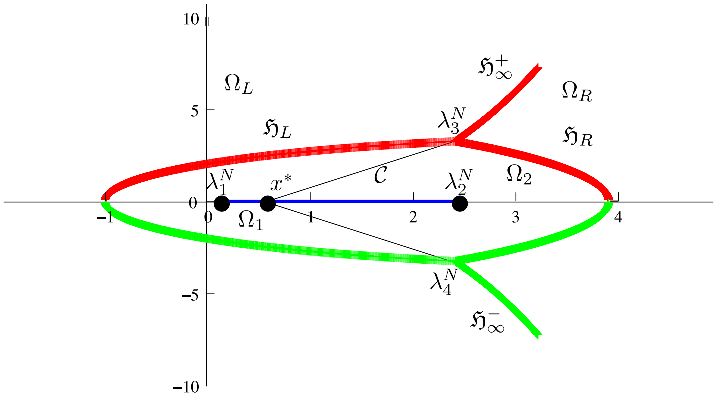

Fig. 3. The set $\mathfrak{H}$ for $a = 0.9$, $\beta_N = 0.7$ and $c_N = 0.4$. The branch points are given by $\lambda_1^N \approx 0.12518$, $\lambda_2^N \approx 2.48841$, $\lambda_3^N \approx 2.40520 + 3.2516i$ and $\lambda_4^N \approx 2.40520 - 3.2516i$. The point ι in Lemma 9 is given by $\iota \approx 0.602$. The function $\mathrm{Re}\left(\theta_2^N(z) - \theta_3^N(z)\right)$ is negative in the open region Ω_L on the left of $\mathfrak{H}_L$ and positive in the region Ω_R on the right hand side of $\mathfrak{H}_R$.

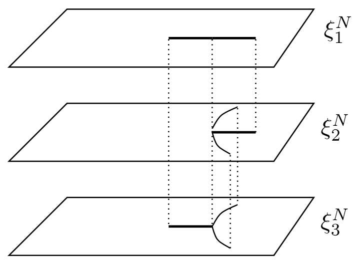

Fig. 4. The branch cut structure of the Riemann surface $\mathcal{L}_N$.

The shape of the set $\mathfrak{H}$ is indicated in Fig. 3. The Octave generated figure shows the set for $a = 0.9$, $\beta_N = 0.7$ and $c_N = 0.4$.

From now on, we will choose the branch cut $\mathcal{C}$ to be a simple curve joining λ_3^N and λ_4^N that is symmetric with respect to the real axis. We also require $\mathcal{C}$ to lie between the curves $\mathfrak{H}_L$ and $\mathfrak{H}_R$ in Proposition 6 and to intersect $\mathbb{R}$ at a point $\lambda_1^N < x^* < \lambda_2^N$. The integration contours for the functions $\theta_j^N(z)$ in (3.21) are chosen such that they do not intersect the set $(-\infty, \lambda_2^N) \cup \mathcal{C}$, and the point λ_l^N in (3.21) is chosen to be λ_2^N. Then by using a similar argument in the proof of Proposition 4, we obtain the following proposition.

Proposition 7. *The point λ_1^N is a branch point of $\xi_3^N(z)$ while λ_2^N is a branch point of $\xi_2^N(z)$.*

We can now determine the jump discontinuities of ξ_j^N on the branch cuts

$$\begin{aligned} &\xi_{1,\pm}^N(z) = \xi_{2,\mp}^N(z), \quad z \in \mathfrak{B}_2, \qquad \xi_{1,\pm}^N(z) = \xi_{3,\mp}^N(z), \quad z \in \mathfrak{B}_3, \\ &\xi_{2,\pm}^N(z) = \xi_{3,\mp}^N(z), \quad z \in \mathcal{C} \end{aligned} \tag{3.26}$$

where $\mathfrak{B}_j$ are defined by

$$\mathfrak{B}_2 = (x^*, \lambda_2^N], \qquad \mathfrak{B}_3 = [\lambda_1^N, x^*). \tag{3.27}$$

The branch cut structure of the Riemann surface $\mathcal{L}_N$ is indicated in Fig. 4.

Finally, let us define $\tilde{\theta}_j^N(z)$ to be constant shifts of the $\theta_j^N(z)$.

$$\begin{aligned} &\tilde{\theta}_1^N(z) = \theta_1^N(z), \qquad \tilde{\theta}_2^N(z) = \theta_2^N(z) - \theta_{2,+}^N(\lambda_2^N), \\ &\tilde{\theta}_3^N(z) = \theta_3^N(z) - \theta_{3,+}^N(\lambda_1^N) + \theta_{1,-}^N(\lambda_1^N). \end{aligned} \tag{3.28}$$

These functions will be used in Section 4 to transform the Riemann–Hilbert problem for the multiple Laguerre polynomials.

3.5. Modification of the Riemann surface in the double scaling limit

In the case when $\Delta(a, \beta_N, c_N) = O\left(M^{-\frac{1}{2}}\right)$, a modification of the functions ξ is needed for the implementation of the Riemann–Hilbert analysis. In this section we will generalize the method in [19] to modify the functions ξ in (1.23). As in the

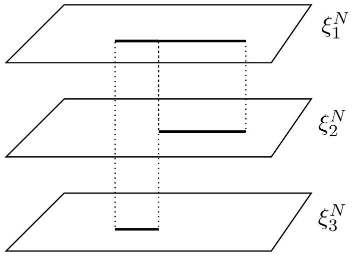

Fig. 5. The branch cut structure of the Riemann surface $\mathcal{L}$ when $\Delta = 0$.

Introduction, let a_0, β_0 and c_0 be the solutions of (1.14) and (1.15), γ_1 and γ_2 be the distinct solutions of (1.6) with parameters a_0, β_0 and c_0, and γ_* be the double root. Let λ_1, λ_2 and λ_* be the images of γ_1, γ_2 and γ_* under the map $z(\xi)$. Let ξ_0 be the solutions of (1.5) with parameters a_0, β_0 and c_0 and behavior (1.23). Then ξ_0 behaves as follows near the point $z = \lambda_*$.

$$\xi_0 = \gamma_* + \rho_*(z-\lambda_*)^{\frac{1}{3}}\left(1 + O\left((z-\lambda)^{\frac{1}{3}}\right)\right), \quad z \to \lambda_*, \tag{3.29}$$

where ρ_* is defined in (1.17). Hence near λ_*, there is only one real solution of (1.5). In particular, λ_* must lie between λ_1 and λ_2, and the Riemann surface $\mathcal{L}$ has the sheet structure as indicated in Fig. 5.

Let us define $\phi(\xi_0)$ to be the following function on the Riemann surface $\mathcal{L}$.

$$\phi(\xi_0) = \frac{\xi_0^2(\xi_0+1)\left(\mathcal{A}_2\xi_0^2 + \mathcal{A}_1\xi_0 + \mathcal{A}_0\right)}{(\xi_0-\gamma_1)(\xi_0-\gamma_2)(\xi_0-\gamma_*)^2}, \tag{3.30}$$

where $\mathcal{A}_j$ are defined by (1.16). Note that ϕ is of order $O(M^{-\frac{1}{2}})$ by (1.18). Then by using the observation that the total residue of differential form $\xi_0 dz$ on $\mathcal{L}$ is zero, together with the fact that γ_1, γ_2 and γ_* are the zeros of the polynomial (1.6), we see that the function $\phi(\xi_0)$ behaves as follows at the points of $z = \infty$ on different sheets of $\mathcal{L}$.

$$\begin{aligned}
&\phi(z) = O(z^{-2}), \quad z \to \infty \text{ on sheet 1}, \\
&\phi(z) = \frac{c_N(1-\beta_N) - c_0(1-\beta_0)}{z} + O(z^{-2}), \quad z \to \infty \text{ on sheet 2}, \\
&\phi(z) = -\frac{1}{a} + \frac{1}{a_0} + \frac{c_N\beta_N - c_0\beta_0}{z} + O(z^{-2}), \quad z \to \infty \text{ on sheet 3},
\end{aligned} \tag{3.31}$$

together with the following singularity at $z = 0$ on the first sheet.

$$\phi(z) = \frac{c_N - c_0}{z} + O(1). \tag{3.32}$$

Due to (1.15), the function ϕ behaves as

$$\phi(z) = \frac{\gamma_*^2\,(\gamma_*+1)\,(2\mathcal{A}_2\gamma_* + \mathcal{A}_1)}{\rho_*\,(\gamma_*-\gamma_1)\,(\gamma_*-\gamma_2)}(z-\lambda_*)^{-\frac{1}{3}} + O(1), \quad z \to \lambda_*. \tag{3.33}$$

Let $\xi_{0,j}$ be the different branches of ξ_0 and let $\xi_j^N = \xi_{0,j}(z) + \phi(\xi_{0,j}(z))$. Define $\tilde{\theta}_j^N(z)$ by

$$\tilde{\theta}_1^N(z) = \int_{\lambda_2}^{z} \xi_1^N(x)dx, \qquad \tilde{\theta}_2^N(z) = \int_{\lambda_2}^{z} \xi_2^N(x)dx, \qquad \tilde{\theta}_3^N(z) = \int_{\lambda_*}^{z} \xi_3^N(x)dx + \int_{\lambda_2}^{\lambda_*} \xi_{1,-}^N(x)dx \tag{3.34}$$

where the path of integration is chosen such that it does not intersect the interval $(-\infty, \lambda_2)$.

Then there exist functions $f_j(z)$ that are conformal within a small enough disc D_* around λ_* such that

$$\begin{aligned}
&\tilde{\theta}_j^N(z) = \begin{cases} \displaystyle\sum_{k=2}^{4} \omega^{2kj} f_k(z)|z-\lambda_*|^{\frac{k}{3}} + \tilde{\theta}_{j,+}^N(\lambda_*), & \mathrm{Im}(z) > 0; \\ \displaystyle\sum_{k=2}^{4} \omega^{kj} f_k(z)|z-\lambda_*|^{\frac{k}{3}} + \tilde{\theta}_{j,-}^N(\lambda_*), & \mathrm{Im}(z) < 0. \end{cases}, \quad j = 1, 2, \\
&\tilde{\theta}_3^N(z) = \begin{cases} \displaystyle\sum_{k=2}^{4} f_k(z)|z-\lambda_*|^{\frac{k}{3}} + \tilde{\theta}_{1,-}^N(\lambda_*), & \mathrm{Im}(z) > 0; \\ \displaystyle\sum_{k=2}^{4} f_k(z)|z-\lambda_*|^{\frac{k}{3}} + \tilde{\theta}_{1,-}^N(\lambda_*), & \mathrm{Im}(z) < 0 \end{cases}
\end{aligned} \tag{3.35}$$

where $\omega = e^{i\frac{2\pi}{3}}$. Note that f_2 is of order $O\left((z-\lambda_*)\right) + O\left(M^{-\frac{1}{2}}\right)$.

By a residue calculation, we see that

$$\tilde{\theta}^N_{1,+}(\lambda_*) - \tilde{\theta}^N_{1,-}(\lambda_*) = -2c_N(1-\beta_N)\pi\mathrm{i}. \tag{3.36}$$

Also, since $\xi_2^N = \overline{\xi}_1^N$ on $[\lambda_*, \lambda_2]$, we have $\tilde{\theta}^N_2(\lambda_*) = \overline{\tilde{\theta}^N_1(\lambda_*)}$. Hence all the constant terms in (3.35) have the same real part.

The functions $\tilde{\theta}^N_j(z)$ will then be used as in [19] to transform the Riemann–Hilbert problem of the multiple Laguerre polynomials.

4. Riemann–Hilbert analysis

We can now implement the Riemann–Hilbert method to obtain the strong asymptotics for the multiple Laguerre polynomials introduced in Section 2 and use it to prove Theorem 1. The analysis is very similar to those in [22,23,19] (see also [20]).

Let $C(f)$ be the Cauchy transform of the function $f(z) \in L^2(\mathbb{R}_+)$ in $\mathbb{R}_+$

$$C(f)(z) = \frac{1}{2\pi\mathrm{i}}\int_{\mathbb{R}_+}\frac{f(s)}{s-z}\mathrm{d}s, \tag{4.1}$$

and let $w_1(z)$ and $w_2(z)$ be the weights of the multiple Laguerre polynomials.

$$w_1(z) = z^{M-N}\mathrm{e}^{-Mz}, \qquad w_2(z) = z^{M-N}\mathrm{e}^{-Ma^{-1}z}. \tag{4.2}$$

Denote by κ_1 and κ_2 the constants

$$\kappa_1 = -2\pi\mathrm{i}\left(h^{(1)}_{N_0-1,N_1}\right)^{-1}, \qquad \kappa_2 = -2\pi\mathrm{i}\left(h^{(2)}_{N_0,N_1-1}\right)^{-1}.$$

Then due to the orthogonality condition (2.1), the following matrix

$$Y(z) = \begin{pmatrix} L_{N_0,N_1}(z) & C(L_{N_0,N_1}w_1)(z) & C(L_{N_0,N_1}w_2)(z) \\ \kappa_1 L_{N_0-1,N_1}(z) & \kappa_1 C(L_{N_0-1,N_1}w_1)(z) & \kappa_1 C(L_{N_0-1,N_1}w_2)(z) \\ \kappa_2 L_{N_0,N_1-1}(z) & \kappa_2 C(L_{N_0,N_1-1}w_1)(z) & \kappa_2 C(L_{N_0,N_1-1}w_2)(z) \end{pmatrix} \tag{4.3}$$

is the unique solution of the following Riemann–Hilbert problem.

$$\begin{aligned} &1.\quad Y(z) \text{ is analytic in } \mathbb{C}\setminus\mathbb{R}_+,\\ &2.\quad Y_+(z) = Y_-(z)\begin{pmatrix}1 & w_1(z) & w_2(z)\\ 0 & 1 & 0\\ 0 & 0 & 1\end{pmatrix}, \quad z\in\mathbb{R}_+\\ &3.\quad Y(z) = \left(I+O(z^{-1})\right)\begin{pmatrix} z^N & 0 & 0\\ 0 & z^{-N_0} & 0\\ 0 & 0 & z^{-N_1}\end{pmatrix}, \quad z\to\infty,\\ &4.\quad Y(z) = O(1), \quad z\to 0. \end{aligned} \tag{4.4}$$

By a similar computation as the one in [32,17], we can express the kernel (2.5) in terms of the solution of the Riemann–Hilbert problem $Y(z)$.

$$\begin{aligned} K_{M,N}(x,y) &= \frac{(xy)^{\frac{M-N}{2}}\left(\mathrm{e}^{-My}\left[Y_+^{-1}(y)Y_+(x)\right]_{21} + \mathrm{e}^{-Ma^{-1}y}\left[Y_+^{-1}(y)Y_+(x)\right]_{31}\right)}{2\pi\mathrm{i}(x-y)},\\ &= \frac{(xy)^{\frac{M-N}{2}}}{2\pi\mathrm{i}(x-y)}\begin{pmatrix}0 & \mathrm{e}^{-My} & \mathrm{e}^{-Ma^{-1}y}\end{pmatrix} Y_+^{-1}(y)Y_+(x)\begin{pmatrix}1\\0\\0\end{pmatrix} \end{aligned} \tag{4.5}$$

where A_{21} and A_{31} are the 21th and 31th entries of A.

4.1. Transformation of the Riemann–Hilbert problem

We will now start deforming the Riemann–Hilbert problem (4.4). First let us define the functions $g_j^N(z)$ to be

$$g_1^N(z) = \tilde{\theta}^N_1(z) + (1-c_N)\log z, \qquad g_2^N(z) = \tilde{\theta}^N_2(z) + z, \qquad g_3^N(z) = \tilde{\theta}^N_3(z) + \frac{z}{a}, \tag{4.6}$$

where $\tilde{\theta}_j^N(z)$ is defined in (3.20), (3.28) and (3.34) and the branch cut of $\log z$ in $g_1^N(z)$ is chosen to be the negative real axis.

We then define $T(z)$ to be

$$T(z) = \operatorname{diag}\left(e^{-Ml_1^N}, e^{-M\tilde{l}_2^N}, e^{-M\tilde{l}_3^N}\right) Y(z) \operatorname{diag}\left(e^{Mg_1^N(z)}, e^{Mg_2^N(z)}, e^{Mg_3^N(z)}\right), \tag{4.7}$$

where $\tilde{l}_2^N$ and $\tilde{l}_3^N$ are given by

$$\tilde{l}_2^N = l_2^N, \qquad \tilde{l}_3^N = l_3^N + \theta_{1,-}^N(\lambda_{\max}^N)$$

for the 2 cut case and the critical case, where $\lambda_{\max}^N$ is the largest λ_j^N, and by

$$\tilde{l}_2^N = l_2^N - \theta_{2,+}^N(\lambda_2^N), \qquad \tilde{l}_3^N = l_3^N(z) - \theta_{3,+}^N(\lambda_1^N) + \theta_{1,-}^N(\lambda_1^N)$$

for the 1 cut case.

The matrix $T(z)$ then satisfies the following Riemann–Hilbert problem.

$$\begin{aligned} &1.\quad T(z) \text{ is analytic in } \mathbb{C} \setminus \mathbb{R},\\ &2.\quad T_+(z) = T_-(z) J_T(z), \quad z \in \mathbb{R},\\ &3.\quad T(z) = I + O(z^{-1}), \quad z \to \infty,\\ &4.\quad T(z) = O(1), \quad z \to 0, \end{aligned} \tag{4.8}$$

where $J_T(z)$ is the following matrix

$$J_T(z) = \begin{pmatrix} e^{M\left(\tilde{\theta}_{1,+}^N(z) - \tilde{\theta}_{1,-}^N(z)\right)} & e^{M\left(\tilde{\theta}_{2,+}^N(z) - \tilde{\theta}_{1,-}^N(z)\right)} & e^{M\left(\tilde{\theta}_{3,+}^N(z) - \tilde{\theta}_{1,-}^N(z)\right)} \\ 0 & e^{M\left(\tilde{\theta}_{2,+}^N(z) - \tilde{\theta}_{2,-}^N(z)\right)} & 0 \\ 0 & 0 & e^{M\left(\tilde{\theta}_{3,+}^N(z) - \tilde{\theta}_{3,-}^N(z)\right)} \end{pmatrix}. \tag{4.9}$$

The matrix $T(z)$ can now be transformed and approximated by using the methods developed in [22,23,19] (see also [20]) to obtain an asymptotic expression for the kernel (4.5). The asymptotic expression can then be used to obtain the results in Theorems 1 and 2. Since the analysis for the non-critical case is fairly standard and well documented, we shall not repeat the details here, but readers who are interested in it can consult the references [22,23,20]. However, in the critical case where $\Delta = O\left(M^{-\frac{1}{2}}\right)$, the error analysis in the Riemann–Hilbert approach needs to be dealt with in a more delicate manner. We shall discuss this case here.

4.2. Lens opening in the critical case

The second transformation to the Riemann–Hilbert problem is the same as the ones in the non-critical 2 cut case. First note that, since the sheet structure of our Riemann surface in Fig. 5 is the same as the one in [19] and the correction term from $\phi(z)$ is of order $O\left(\frac{(z-\lambda_*)^{\frac{2}{3}}}{M^{\frac{1}{2}}}\right)$, we have the following.

Lemma 11. *Let D_1 and D_2 be small disc centers at λ_1 and λ_2 with a small radius independent of M, and D_* a small disc center at λ_* with radius $M^{-\frac{1}{2}}$ and let $\mathfrak{B}_2 = [\lambda_*, \lambda_2]$ and $\mathfrak{B}_3 = [\lambda_1, \lambda_*]$. Then the real parts of $\tilde{\theta}_j^N(z)$ are continuous across $\mathbb{R}$ and for large enough M, we have the following*

$$\mathrm{Re}(\tilde{\theta}_1^N(z)) > \mathrm{Re}(\tilde{\theta}_j^N(z)), \quad x \in \mathbb{R}_+ \setminus \left(\mathfrak{B}_j \cup D\right) \tag{4.10}$$

and there exist neighborhoods U_j of the interval $\mathfrak{B}_j$ in $\mathbb{C}$ such that

$$\mathrm{Re}(\tilde{\theta}_j^N(z)) > \mathrm{Re}(\tilde{\theta}_1(z)) > \mathrm{Re}(\tilde{\theta}_k^N(z)), \quad z \in U_j \setminus D,\ j = 2, 3, \tag{4.11}$$

where $k = 2, 3$, $k \neq j$ and $D = D_1 \cup D_2 \cup D_*$.

We also have the following lemma concerning the jump discontinuities of the $\tilde{\theta}_j^N$.

Lemma 12. *The integral $\tilde{\theta}_1^N(z)$ is analytic on $\mathbb{C} \setminus (-\infty, \lambda_2]$ and continuous up to $\mathbb{R} \setminus \{0\}$. The integrals $\tilde{\theta}_2^N(z)$ and $\tilde{\theta}_3^N(z)$ are analytic on $\mathbb{C} \setminus (-\infty, \lambda_2]$ and $\mathbb{C} \setminus (-\infty, \lambda_*]$ respectively and are continuous up to $\mathbb{R}$. Across the real axis, they have the following jump discontinuities.*

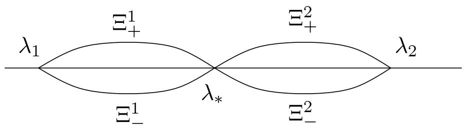

Fig. 6. The lens contours.

$$
\begin{aligned}
&\tilde{\theta}^N_{1,\pm}(z) = \tilde{\theta}^N_{j,\mp}(z), \quad z \in \mathfrak{B}_j,\\
&\tilde{\theta}^N_{1,+}(z) = \tilde{\theta}^N_{1,-}(z) - 2c_N\pi\mathrm{i}, \quad z \in (0, \lambda_1],\\
&\tilde{\theta}^N_{1,+}(z) = \tilde{\theta}^N_{1,-}(z) - 2\pi\mathrm{i}, \quad z \in (-\infty, 0),\\
&\tilde{\theta}^N_{2,+}(z) = \tilde{\theta}^N_{2,-}(z) + 2c_N(1-\beta_N)\pi\mathrm{i}, \quad z \in (-\infty, \lambda_*],\\
&\tilde{\theta}^N_{3,+}(z) = \tilde{\theta}^N_{3,-}(z) + 2c_N\beta_N\pi\mathrm{i}, \quad z \in (-\infty, \lambda_1].
\end{aligned}
\tag{4.12}
$$

These two lemmas follow from the relative sizes of $\mathrm{Re}(\xi_{0,j})$ and the jump discontinuities (3.18) of $\xi^N_j(z)$ (with $\lambda^N_2 = \lambda^N_3 = \lambda_*$) on $\mathbb{R}$ and are straightforward to verify. We shall not give the proof here but refer the readers to [22,20].

We can now define the lens contours as in Fig. 6 and define the matrix $S(z)$ to be

$$
S(z) = \begin{cases} T(z), & z \text{ outside the lens regions;}\\ T(z)K^{-1}_{j,+}(z), & z \text{ in the upper lens region of } \mathfrak{B}_j;\\ T(z)K_{j,-}(z), & z \text{ in the lower lens region of } \mathfrak{B}_j; \end{cases}
\tag{4.13}
$$

where $K_{j,\pm}(z)$ are

$$
\begin{aligned}
K_{2,\pm}(z) &= \begin{pmatrix} 1 & 0 & 0\\ \mathrm{e}^{M\left(\tilde{\theta}^N_1(z)-\tilde{\theta}^N_2(z)\right)} & 1 & \pm\mathrm{e}^{M\left(\tilde{\theta}^N_3(z)-\tilde{\theta}^N_2(z)\right)}\\ 0 & 0 & 1 \end{pmatrix},\\
K_{3,\pm}(z) &= \begin{pmatrix} 1 & 0 & 0\\ 0 & 1 & 0\\ \mathrm{e}^{M\left(\tilde{\theta}^N_1(z)-\tilde{\theta}^N_3(z)\right)} & \pm\mathrm{e}^{M\left(\tilde{\theta}^N_2(z)-\tilde{\theta}^N_3(z)\right)} & 1 \end{pmatrix}.
\end{aligned}
\tag{4.14}
$$

Then by using Lemma 12, we see that the matrix $S(z)$ is a solution to the following Riemann–Hilbert problem.

$$
\begin{aligned}
&1.\quad S(z) \text{ is analytic in } \mathbb{C} \setminus \left(\mathbb{R}_+ \cup \Xi^j_\pm\right),\\
&2.\quad S_+(z) = S_-(z)J_S(z), \quad z \in \left(\mathbb{R}_+ \cup \Xi^j_\pm\right),\\
&3.\quad S(z) = I + O(z^{-1}), \quad z \to \infty,\\
&4.\quad S(z) = O(1), \quad z \to 0.
\end{aligned}
\tag{4.15}
$$

On $\mathfrak{B}_2$ and $\mathfrak{B}_3$, the matrix J_S is given by

$$
J_S(z) = \begin{pmatrix} 0 & 1 & 0\\ -1 & 0 & 0\\ 0 & 0 & 1 \end{pmatrix}, \quad z \in \mathfrak{B}_2, \qquad J_S(z) = \begin{pmatrix} 0 & 0 & 1\\ 0 & 1 & 0\\ -1 & 0 & 0 \end{pmatrix}, \quad z \in \mathfrak{B}_3
\tag{4.16}
$$

and on $\Xi^j_\pm$, it is given by $J_S(z) = K_{j,\pm}(z)$ for $z \in \Xi^j_\pm$. On $\mathbb{R}_+ \setminus \left(\bigcup_{j=1}^2 [\lambda^N_{k_j-1}, \lambda^N_{k_j}]\right)$, we have $J_S(z) = J_T(z)$.

Then by Lemma 11, we see that, away from $\mathfrak{B}_j$ and from some small neighborhoods D_j and D_* of λ_j and λ_*, the off-diagonal entries of $J_S(z)$ are exponentially small as $M \to \infty$. This suggests the following approximation to the Riemann–Hilbert problem (4.15).

$$
\begin{aligned}
&1.\quad S^\infty(z) \text{ is analytic in } \mathbb{C} \setminus \left(\bigcup_{j=2}^3 \mathfrak{B}_j\right),\\
&2.\quad S^\infty_+(z) = S^\infty_-(z)J_S(z), \quad z \in \bigcup_{j=2}^3 \mathfrak{B}_j,\\
&3.\quad S^\infty(z) = I + O(z^{-1}), \quad z \to \infty.
\end{aligned}
\tag{4.17}
$$

The solution of this Riemann–Hilbert problem is known as the ‘outer parametrix’. It can be constructed by using an algebraic function on the Riemann surface $\mathcal{L}$ as in [19]. This is given as follows. Let Γ_j be the images of $\mathfrak{B}_j$ on $\mathcal{L}$ under the map $\xi_{0,1,+}(z)$.

That is,

$$\Gamma_j = \left\{(z,\xi) \in \mathcal{L} \mid \xi = \xi_{0,1,+}(z),\ z \in \mathfrak{B}_j\right\}, \quad j = 2, 3. \tag{4.18}$$

Let us now define the functions $S_k^{\infty}(\xi)$, $k = 1, 2, 3$ to be the following functions on $\mathcal{L}$.

$$\begin{aligned} S_1^{\infty}(\xi) &= a\gamma_* \sqrt{\prod_{j=1}^{2}\gamma_j}\, \frac{(\xi+1)(\xi+a^{-1})}{\sqrt{\prod_{j=1}^{2}(\xi-\gamma_j)(\xi-\gamma_*)^2}}, \\ S_2^{\infty}(\xi) &= \frac{a\sqrt{\prod_{j=1}^{2}(1+\gamma_*)^2(1+\gamma_j)}}{a-1}\, \frac{\xi(\xi+a^{-1})}{\sqrt{\prod_{j=1}^{2}(\xi-\gamma_j)(\xi-\gamma_*)^2}}, \\ S_3^{\infty}(\xi) &= \frac{\sqrt{\prod_{j=1}^{2}(1+\gamma_*)^2(1+a\gamma_j)}}{1-a}\, \frac{\xi(\xi+1)}{\sqrt{\prod_{j=1}^{2}(\xi-\gamma_j)(\xi-\gamma_*)^2}}. \end{aligned} \tag{4.19}$$

The branch cuts of the square root in (4.19) are chosen to be the contours Γ_j (4.18). Then the matrix $S^{\infty}(z)$ with entries $S_{ij}^{\infty}(z) = S_i^{\infty}(\xi_{0,j}(z))$, $i, j = 1, 2, 3$ will satisfy the Riemann–Hilbert problem (4.17).

4.3. Local parametrices

Near the edge points λ_1, λ_2 and λ_*, the approximation of $S(z)$ by $S^{\infty}(z)$ failed and we must solve the Riemann–Hilbert problem exactly near these points and match the solutions to the outer parametrix $S^{\infty}(z)$ up to an error term that vanishes as $M \to \infty$. To be precise, let D_k and D_* be small disc centers at the points λ_k and λ_*. We would like to construct local parametrices $S^p(z)$ in these discs D such that

$$\begin{aligned} &1.\quad S^p(z) \text{ is analytic in } D \setminus \left(\mathbb{R} \cup \Xi_-^k \cup \Xi_+^k\right), \\ &2.\quad S_+^p(z) = S_-^p(z) J_S(z), \quad z \in D \cap \left(\mathbb{R} \cup \Xi_-^k \cup \Xi_+^k\right), \\ &3.\quad S^p(z) = S^{\infty}(z)\left(I + o(1)\right), \quad z \in \partial D. \end{aligned} \tag{4.20}$$

The local parametrices $S^k(z)$ at the edge point λ_k can be constructed by using the Airy function as in [22,20]. Since the construction is identical to the one in [22,20], we shall not give the details here but will concentrate on the new feature that arises in the construction of the local parametrix near λ_*.

4.3.1. The neighborhood D_* and a conformal map

Let us now define the neighborhood D_* to be the disc of radius $M^{-\frac{1}{2}}$ center at λ_*.

Let us now define conformal maps ζ and t inside D_* to be

$$\zeta = \left(\frac{4}{3}f_4(z)\right)^{\frac{3}{4}}(z-\lambda_*), \qquad t(z) = \frac{\sqrt{3}f_2(z)}{f_4^{\frac{1}{2}}(z)}, \tag{4.21}$$

where f_4 and f_2 are the conformal maps defined in (3.35). Note that, as remarked after (3.35), f_2 is of order $O\left((z-\lambda_*)\right) + O\left(M^{-\frac{1}{2}}\right)$. Therefore when $|z-\lambda_*| = O(M^{-\frac{3}{4}})$, $t(z)$ is of order

$$t(z) = M^{-\frac{1}{2}}\left(t_0 + O\left(M^{-\frac{1}{4}}\right)\right)$$

where t_0 is defined in Theorem 2. Moreover, $M^{\frac{1}{2}}t(z)$ is bounded in D_*. The map ζ will map the neighborhood D_* into the complex ζ plane with ∂D_* approaching infinity as $M \to \infty$.

Remark 1. In [19], the $z - \lambda_*$ term in the function $f_2(z)$ vanishes and $f_2(z)$ is of order $O(M^{-\frac{1}{2}}) + O\left((z-\lambda_*)^2\right)$. This is a special property of the problem considered in [19]. As a result, $M^{\frac{1}{2}}t(z)$ is bounded inside a bigger disc of radius $M^{-\frac{1}{4}}$. In our case, this may not be true and we have to use the smaller disc of radius $M^{-\frac{1}{2}}$, which leads to a larger error term and the error analysis has to be dealt with in a different way.

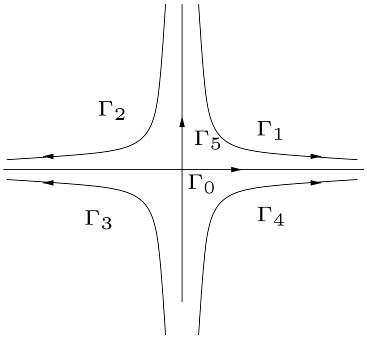

Fig. 7. Contours Γ_j in the definition of the Pearcey integrals.

4.3.2. Pearcey integrals

First note that under the conformal map ζ, the contours $\mathfrak{B}_2$ and $\mathfrak{B}_3$ are mapped into $\mathbb{R}_+$ and $\mathbb{R}_-$ respectively. Let us now deform the lens contours inside D_* such that under the map ζ, $\Xi_\pm^2$ are mapped into the rays $\arg(\zeta) = \pm\frac{\pi}{4}$ and $\Xi_\pm^3$ are mapped into the rays $\arg(\zeta) = \pm\frac{3\pi}{4}$. Let G be the diagonal matrix $G = \operatorname{diag}\left(\tilde{\theta}_1^N, \tilde{\theta}_2^N, \tilde{\theta}_3^N\right)$. Then the matrix $\hat{S}(z) = S(z)e^{-MG(z)}$ will have the following jump discontinuities inside D_*.

$$\begin{aligned}
&\hat{S}_+(z) = \hat{S}_-(z)J_{\hat{S}}(z), \quad J_{\hat{S}} = J_S, \quad z \in \mathfrak{B}_j, \quad j = 2, 3 \\
&J_{\hat{S}} = \begin{pmatrix} 1 & 0 & 0 \\ 1 & 1 & \pm 1 \\ 0 & 0 & 1 \end{pmatrix}, \quad z \in \Xi_\pm^2, \qquad J_{\hat{S}} = \begin{pmatrix} 1 & 0 & 0 \\ 0 & 1 & 0 \\ 1 & \pm 1 & 1 \end{pmatrix}, \quad z \in \Xi_\pm^3.
\end{aligned} \tag{4.22}$$

The matrix with the above jump discontinuities can be constructed using the Pearcey integrals as in [19].

$$p_j(\zeta) = \int_{\Gamma_j} e^{-\frac{s^4}{4} - \frac{t}{2}s^2 + is\zeta} ds, \quad j = 0, \dots, 5, \tag{4.23}$$

where the contours Γ_j are

$$\begin{aligned}
&\Gamma_0 = (-\infty, \infty), && \Gamma_1 = (i\infty, 0] \cup [0, \infty), \\
&\Gamma_2 = (i\infty, 0] \cup [0, -\infty), && \Gamma_3 = (-i\infty, 0] \cup [0, -\infty), \\
&\Gamma_4 = (-i\infty, 0] \cup [0, \infty), && \Gamma_5 = i\mathbb{R},
\end{aligned} \tag{4.24}$$

or homotopic deformations such as the ones shown Fig. 7. We also equip each Γ_j with an orientation as shown in Fig. 7. Let us denote the rays L_j by $L_0 = L_6 = \mathbb{R}_+$, $L_1 = e^{i\frac{\pi}{4}}L_0$, $L_2 = e^{i\frac{3\pi}{4}}L_0$, $L_3 = \mathbb{R}_-$, $L_4 = e^{-i\frac{3\pi}{4}}L_0$ and $L_5 = e^{-i\frac{\pi}{4}}L_0$. Let the region Ω_j be the region between L_{j-1} and L_j for $j = 1, \dots, 6$. Now let the matrix $\Phi(\zeta, t)$ be $\Phi(\zeta, t) = \Phi_j(\zeta)$ for $\zeta \in \Omega_j$, where $\Phi_j(\zeta)$ is given by

$$\begin{aligned}
&\Phi_1(\zeta) = \begin{pmatrix} -p_2 & p_1 & p_5 \\ -p_2' & p_1' & p_5' \\ -p_2'' & p_1'' & p_5'' \end{pmatrix}, \qquad \Phi_2(\zeta) = \begin{pmatrix} p_0 & p_1 & p_4 \\ p_0' & p_1' & p_4' \\ p_0'' & p_1'' & p_4'' \end{pmatrix}, \qquad \Phi_3(\zeta) = \begin{pmatrix} -p_3 & -p_5 & p_4 \\ -p_3' & -p_5' & p_4' \\ -p_3'' & -p_5'' & p_4'' \end{pmatrix}, \\
&\Phi_4(\zeta) = \begin{pmatrix} p_4 & -p_5 & p_3 \\ p_4' & -p_5' & p_3' \\ p_4'' & -p_5'' & p_3'' \end{pmatrix}, \qquad \Phi_5(\zeta) = \begin{pmatrix} p_0 & p_2 & p_3 \\ p_0' & p_2' & p_3' \\ p_0'' & p_2'' & p_3'' \end{pmatrix}, \qquad \Phi_6(\zeta) = \begin{pmatrix} p_1 & p_2 & p_5 \\ p_1' & p_2' & p_5' \\ p_1'' & p_2'' & p_5'' \end{pmatrix}.
\end{aligned}$$

Then, as in [19], the matrix $\Phi(\zeta, t)$ will satisfy the jump discontinuities (4.22). Moreover, it has the following behavior as $\zeta \to \infty$.

$$\Phi(\zeta, t) = \sqrt{\frac{2\pi}{3}} i e^{\frac{t^2}{8}} Z(\zeta) \begin{pmatrix} \mp\omega & \omega^2 & 1 \\ \mp 1 & 1 & 1 \\ \mp\omega^2 & \omega & 1 \end{pmatrix} \left(I + O(\zeta^{-\frac{2}{3}})\right) \Theta_\pm(\zeta, t), \quad \pm\operatorname{Im}(\zeta) > 0, \tag{4.25}$$

where Z is the diagonal matrix $Z = \operatorname{diag}\left(\zeta^{-\frac{1}{3}}, 1, \zeta^{\frac{1}{3}}\right)$ and $\Theta_\pm$ is the diagonal matrix

$$\Theta_+ = \operatorname{diag}\left(\vartheta_1(\zeta, t), \vartheta_2(\zeta, t), \vartheta_3(\zeta, t)\right), \qquad \Theta_- = \operatorname{diag}\left(\vartheta_2(\zeta, t), \vartheta_1(\zeta, t), \vartheta_3(\zeta, t)\right),$$

where ϑ_j are defined by $\vartheta_j(x, y) = \frac{3}{4}\omega^{2j}x^{\frac{4}{3}} + \omega^j\frac{y}{2}x^{\frac{2}{3}}$. The proof of the jump discontinuities and asymptotic behavior of $\Phi(\zeta, t)$ can be found in Section 8 of [19] and we shall not repeat them here.

4.3.3. Construction of the local parametrix

We will now construct the local parametrix using the matrix $\Phi(\zeta, t)$.

First note that, from (3.35) and (4.21), we have

$$\begin{aligned}\vartheta_j(M^{\frac{3}{4}}\zeta, M^{\frac{1}{2}}t(z)) &= M\tilde{\theta}_j^N(z) - Mf_3(z)(z-\lambda_*) + M\varphi_{j,+}, \quad \mathrm{Im}(z) > 0,\\ \vartheta_j(M^{\frac{3}{4}}\zeta, M^{\frac{1}{2}}t(z)) &= M\tilde{\theta}_{\nu_j}^N(z) - Mf_3(z)(z-\lambda_*) + M\varphi_{\nu_j,-}, \quad \mathrm{Im}(z) < 0,\end{aligned} \tag{4.26}$$

where $\nu_1 = 2$, $\nu_2 = 1$ and $\nu_3 = 3$, and $\varphi_{j,\pm}$ are the constants in (3.35) given by $\varphi_{j,\pm} = \tilde{\theta}_{j,\pm}^N(\lambda_*)$ for $j = 1, 2$ and $\varphi_{3,\pm} = \tilde{\theta}_{1,-}^N(\lambda_*)$. As remarked after (3.35), all these constants have the same real part. Let us denote this real part by $M\varphi$; then from (3.36) and the fact that $\tilde{\theta}_2^N(\lambda_*) = \overline{\tilde{\theta}_1^N(\lambda_*)}$, we have

$$\mathrm{diag}\left(e^{M\varphi_{1,\pm}}, e^{M\varphi_{2,\pm}}, e^{M\varphi_{3,\pm}}\right) = e^{M\varphi}\Psi, \quad \Psi = \mathrm{diag}\left(e^{M\varphi_{1,+}^I}, e^{M\varphi_{2,+}^I}, e^{M\varphi_{3,+}^I}\right), \tag{4.27}$$

where $\varphi_{j,+}^I$ is the imaginary part of $\varphi_{j,+}$.

Let us now define the matrix $E(z)$ to be

$$E(z) = -\sqrt{\frac{3}{2\pi}}\,\mathrm{i}e^{-\mathrm{i}\frac{t^2(z)}{8}} S^{\infty}(z)\Psi^{-1}\begin{pmatrix} \mp\omega & \omega^2 & 1\\ \mp 1 & 1 & 1\\ \mp\omega^2 & \omega & 1\end{pmatrix}^{-1} Z^{-1}(\zeta), \quad \pm\mathrm{Im}(z) > 0. \tag{4.28}$$

Then as in [19], we can verify that $E(z)$ has no jump discontinuities in D_* and has at most a $(z-\lambda_*)^{-\frac{2}{3}}$ singularity at λ_*. Hence this singularity is removable and $E(z)$ is analytic inside D_*. In particular, we see that near λ_*, $S^{\infty}(z)$ can be written as

$$S^{\infty}(z) = S_0\left(I + O(z-\lambda_*)\right)\mathrm{diag}\left((z-\lambda_*)^{-\frac{1}{3}}, 1, (z-\lambda_*)^{\frac{1}{3}}\right)K_{\pm}, \quad \pm\mathrm{Im}(z) > 0 \tag{4.29}$$

for some constant invertible matrices S_0 and $K_{\pm}$ such that $K_{\pm}$ are bounded in M and that $K_+ = K_- J_K$ where J_K is bounded in M also.

Since $\Phi(\zeta, t)$ satisfies the jump discontinuities in (4.22), the matrix $S^*(z)$

$$S^*(z) = E(z)\Phi\left(M^{\frac{3}{4}}\zeta, M^{\frac{1}{2}}t(z)\right)e^{-MG}e^{-M(\varphi - f_3(z-\lambda_*))}, \tag{4.30}$$

where $G = \mathrm{diag}\left(\tilde{\theta}_1^N, \tilde{\theta}_2^N, \tilde{\theta}_3^N\right)$ satisfies the jump discontinuities of $S(z)$ inside D_*. Moreover, from the asymptotic behavior (4.25) of $\Phi(\zeta, t)$, (4.26) and the fact that the entries of Ψ are of unit modulus, we see that near the boundary of D_*, we have

$$S^*(z) = S^{\infty}(z)\left(I + O(M^{-\frac{1}{6}})\right). \tag{4.31}$$

This gives us the local parametrix near λ_*. Note that the error in (4.31) is of order $M^{-\frac{1}{6}}$, which is bigger than the $M^{-\frac{1}{3}}$ error term that appears in [19]. The main problem now is that, as seen from (4.29), the matrix $S^{\infty}(z)$ and its inverse are of order $M^{\frac{1}{6}}$ at the boundary of D_* and hence we do not have the following condition

$$S^*(z) = \left(I + O(M^{-\frac{1}{6}})\right)S^{\infty}(z)$$

that is needed to carry out the usual error analysis. A more delicate method is needed to handle this.

4.4. Final transformation of the Riemann–Hilbert problem

We will show that the parametrices constructed in previous sections are indeed a good approximation to the matrix $S(z)$. As mentioned before, this part of the analysis is different from the ones in [19] due to the larger error term that appeared in (4.31).

Let $S^{(1)}(z)$ and $S^{(2)}(z)$ be the local parametrices at the edge points λ_1 and λ_2. These local parametrices $S^{(1)}(z)$ and $S^{(2)}(z)$ behave as follows at the boundary of D_1 and D_2

$$S^{(j)}(z) = S^{\infty}(z)\left(I + O\left(M^{-1}\right)\right), \quad z \in \partial D_j,\ j = 1, 2, \tag{4.32}$$

while the behavior of the local parametrix $S^*(z)$ at ∂D_* is given by (4.31).

As mentioned before, a more delicate method is needed to analyze the error. We will now adopt a method used by Its and Chen in [33] to achieve this. Let us define the matrix $R(z)$ by the following

$$R(z) = \begin{cases} \Lambda^{-1}S(z)\left(S^{(k)}(z)\right)^{-1}\Lambda, & z \text{ inside } D_k,\ k = 1, 2;\\ \Lambda^{-1}S(z)\left(S^*(z)\right)^{-1}\Lambda, & z \text{ inside } D_*;\\ \Lambda^{-1}S(z)\left(S^{\infty}(z)\right)^{-1}\Lambda, & z \text{ outside } D_1, D_2 \text{ and } D_*\end{cases} \tag{4.33}$$

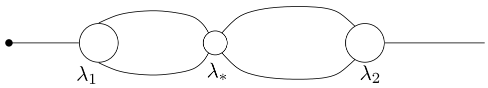

Fig. 8. The jump contour Γ_R of the matrix $R(z)$, where the circles are the boundaries of the discs D_1, D_2 and D_*.

where Λ is the following constant matrix

$$\Lambda = S_0 \mathrm{diag}\left(M^{\frac{1}{6}}, 1, M^{-\frac{1}{6}}\right), \tag{4.34}$$

where S_0 is the matrix in (4.29). Then the matrix $R(z)$ will have jump discontinuities on the contour Γ_R shown in Fig. 8. It will behave like the identity matrix as $z \to \infty$ and by (4.31) and (4.32), we see that the jump matrix $J_R(z)$ of $R(z)$ has the following order of magnitude.

$$J_R(z) = \begin{cases} I + O(M^{-1}), & z \in \partial D_k, k = 1, 2; \\ I + O(M^{-\frac{1}{6}}), & z \in \partial D_*; \\ I + O\left(\mathrm{e}^{-M^{\frac{1}{3}}\eta}\right), & \text{for some fixed } \eta > 0 \text{ on the rest of } \Gamma_R. \end{cases} \tag{4.35}$$

Then by the results in the Appendix of [19], we have

$$R(z) = I + O\left(\frac{1}{M^{\frac{1}{6}}(|z|+1)}\right), \tag{4.36}$$

uniformly in $\mathbb{C}$. This gives us the following asymptotic formula for the matrix $S(z)$.

$$S(z) = \begin{cases} \Lambda\left(I + O\left(M^{-\frac{1}{6}}\right)\right)\Lambda^{-1}S^k(z), & z \in D_k, k = 1, 2; \\ \Lambda\left(I + O\left(M^{-\frac{1}{6}}\right)\right)\Lambda^{-1}S^*(z), & z \in D_*; \\ \Lambda\left(I + O\left(M^{-\frac{1}{6}}\right)\right)\Lambda^{-1}S^\infty(z), & z \text{ outside } D_1, D_2 \text{ and } D_*. \end{cases} \tag{4.37}$$

This completes the Riemann–Hilbert analysis and the proof of the universality theorem (Theorem 2) now follows an identical argument to the ones in [19]. We shall not repeat those details here.

5. Conclusions

In this paper we used the Riemann–Hilbert method to obtain universality results for complex Wishart ensembles in the class $W_{\mathbb{C}}(\Sigma_N, M)$ with a general covariance matrix Σ_N that has 2 distinct eigenvalues. Without loss of generality, we assume that one of these eigenvalues is one and the other is $a < 1$. We also allow the number of each of these eigenvalues to grow with the size of the matrix. In this case, the limiting spectrum of the Wishart matrix can be supported on 1 or 2 intervals. We have computed the asymptotics of the correlation kernel in both these cases and also the phase transition between them. We showed that, as long as the covariance matrix has 2 distinct eigenvalues, the local eigenvalue statistics are given by the sine-kernel (1.11) in the bulk, the Airy kernel (1.12) in the edge, and the Pearcey kernel (1.19) at the critical point of the spectrum. This is similar to the simpler 'Gaussian random matrix with external source' considered by Bleher and Kuijlaars.

The use of Stieltjes transform to provide a Riemann surface needed for the implementation of the Riemann–Hilbert analysis can be generalized to cases where the covariance matrix has more than 2 distinct eigenvalues. In that case, the Riemann surface will be a p-folded covering of the complex plane, where p is the number of distinct eigenvalues. Let $P(\xi, z) = 0$ be the equation of this Riemann surface; then P is a degree p polynomial in ξ and linear in z. Let $\xi_1, \ldots, \xi_p$ be the branches of ξ. When the Riemann surface has complex branch points, the Riemann–Hilbert analysis requires the study of the zero set $\mathfrak{H}$ of the functions $\mathrm{Re}\left(\int\left(\xi_i - \xi_j\right)\mathrm{d}z\right)$, where ξ_i and ξ_j are branched together at a complex branch point. The corresponding analysis of these zero sets for the Gaussian random matrix with an external source was recently done by Orantin in [34]. The analysis uses the fact that ξ_i and ξ_j are only branched together at 2 simple branch points and that the function $\int\left(\xi_i - \xi_j\right)\mathrm{d}z$ behaves as $\kappa\xi + O(1)$ at infinity, for some constant κ. Since these properties are also true for the complex Wishart ensembles, one should be able to apply the method used in [34] to complex Wishart ensembles whose covariance matrix has an arbitrary number of distinct eigenvalues.

Acknowledgments

The author acknowledges A. Kuijlaars for pointing out reference [20] and A. Its for providing a preprint of [33].

References

[1] R. Muirhead, Aspects of Multivariate Statistical Theory, in: Wiley Series in Probability and Mathematical Statistics, 1982.
[2] S. Choi, J. Silverstein, Analysis of the limiting spectral distribution of large-dimensional random matrices, J. Multivariate Anal. 54 (2) (1995) 295–309.
[3] J. Baik, Painlevé formulas of the limiting distributions for nonnull complex sample covariance matrices, Duke Math. J. 133 (2) (2006) 205–235.
[4] J. Baik, G. Ben-Arous, S. Péché, Phase transition of the largest eigenvalue for nonnull complex sample covariance matrices, Ann. Probab. 33 (5) (2005) 1643–1697.
[5] J. Baik, J. Silverstein, Eigenvalues of large sample covariance matrices of spiked population models, J. Multivariate Anal. 97 (6) (2006) 1382–1408.
[6] P. Desrosiers, P.J. Forrester, Asymptotic correlations for Gaussian and Wishart matrices with external source, Int. Math. Res. Not. (2006) 43 pp. Art. ID 27395.
[7] N. El Karoui, On the largest eigenvalue of Wishart matrices with identity covariance when n, p and $p/n \to \infty$. arXiv:math.ST/0309355.
[8] N. El Karoui, Tracy–Widom limit for the largest eigenvalue of a large class of complex sample covariance matrices, Ann. Probab. 35 (2) (2007) 663–714.
[9] P.J. Forrester, The spectrum edge of random matrix ensembles, Nuclear Phys. B 402 (1993) 709–728.
[10] I. Johnstone, On the distribution of the largest principal component, Ann. Statist. 29 (2001) 295–327.
[11] K. Johansson, Shape fluctuations and random matrices, Comm. Math. Phys. 209 (2000) 437–476.
[12] D. Wang, Spiked Models in Wishart Ensemble. arXiv:0804.0889.
[13] D. Wang, The largest sample eigenvalue distribution in the rank 1 quaternionic spiked model of Wishart ensemble, Ann. Probab. 37 (4) (2009) 1273–1328.
[14] E. Brézin, S. Hikami, Correlations of nearby levels induced by a random potential, Nuclear Phys. B 479 (1996) 697–706.
[15] E. Brézin, S. Hikami, Universal singularity at the closure of a gap in a random matrix theory, Phys. Rev. E 57 (1998) 4140–4149.
[16] F. Mezzadri, M.Y. Mo, On an average over the Gaussian Unitary Ensemble, Int. Math. Res. Not. (2009) Article ID rnp062.
[17] P. Bleher, A.B.J. Kuijlaars, Integral representations for multiple Hermite and multiple Laguerre polynomials, Ann. Inst. Fourier (Grenoble) 55 (6) (2005) 2001–2014.
[18] C. Tracy, H. Widom, Level-spacing distribution and the Airy kernel, Comm. Math. Phys. 159 (1994) 151–174.
[19] P. Bleher, A.B.J. Kuijlaars, Large n limit of Gaussian random matrices with external source, III: Double scaling limit, Comm. Math. Phys. 259 (2) (2005) 481–517.
[20] V. Lysov, F. Wielonsky, Strong asymptotics for multiple Laguerre polynomials, Constr. Approx. 28 (2008) 61–111.
[21] C. Tracy, H. Widom, Level spacing distributions and the Bessel kernel, Comm. Math. Phys. 161 (1994) 289–309.
[22] P. Bleher, A.B.J. Kuijlaars, Large n limit of Gaussian random matrices with external source, I, Comm. Math. Phys. 252 (1–3) (2005) 43–76.
[23] A.I. Aptekarev, P. Bleher, A.B.J. Kuijlaars, Large n limit of Gaussian random matrices with external source, II, Comm. Math. Phys. 259 (2005) 367–389.
[24] K.T.R. Mclaughlin, Asymptotic analysis of random matrices with external source and a family of algebraic curves, Nonlinearity 20 (7) (2007) 1547–1571.
[25] Z.D. Bai, J. Silverstein, On the empirical distribution of eigenvalues of a class of large-dimensional random matrices, J. Multivariate Anal. 54 (2) (1995) 175–192.
[26] Z.D. Bai, J. Silverstein, No eigenvalues outside the support of the limiting spectral distribution of large-dimensional sample covariance matrices, Ann. Probab. 26 (1) (1998) 316–345.
[27] Z.D. Bai, J. Silverstein, Exact separation of eigenvalues of large-dimensional sample covariance matrices, Ann. Probab. 27 (3) (1999) 1536–1555.
[28] J. Silverstein, Strong convergence of the empirical distribution of eigenvalues of large-dimensional random matrices, J. Multivariate Anal. 55 (2) (1995) 331–339.
[29] A.I. Aptekarev, Multiple orthogonal polynomials, J. Comput. Appl. Math. 99 (1–2) (1998) 423–447.
[30] A.I. Aptekarev, A. Branquinho, W. Van Assche, Multiple orthogonal polynomials for classical weights, Trans. Amer. Math. Soc. 355 (10) (2003) 3887–3914.
[31] J.S. Geronimon, A.B.J. Kuijlaars, W. Van Assche, Riemann–Hilbert problems for multiple orthogonal polynomials, in: J. Bustoz, M.E.H. Ismail, S.K. Suslov (Eds.), Nato ASI Special Function 2000. Current Perspective and Future Directions, in: Nato Science Series II, vol. 30, Kluwer Academic Publishers, 2001, pp. 23–59.
[32] P. Bleher, A.B.J. Kuijlaars, Random matrices with external source and multiple orthogonal polynomials, Int. Math. Res. Not. (3) (2004) 109–129.
[33] A. Its, Y. Chen, Painlevé III and a singular linear statistics in Hermitian random matrix ensembles II. The asymptotic analysis (in preparation).
[34] N. Orantin, Gaussian matrix model in an external field and non-intersecting Brownian motions. arXiv:0803.0705.